الجمهورية الجزائرية الديمقراطية الشعبية

République Algérienne Démocratique et Populaire

وزارة التعليم العالي و البحث العلمي

Ministère de l'enseignement supérieur et de la recherche scientifique

Université Mohamed Khider – Biskra
Faculté des Sciences et de la Technologie
Département : Génie Electrique
Ref :……

جامعة محمد خيضربسكرة
كلية العلوم و التكنولوجيا
قسم: الهندسة الكهربائية
المرجع : .....

Thèse présentée en vue de l'obtention

Du diplôme de

Doctorat LMD en : Automatique

Option : Modélisation et Contrôle des Systèmes Dynamique

Commande Neuro-Floue d'un bras Manipulateur par les Signaux Electro-Myographiques (EMG)

Neuro-Fuzzy Control of a Manipulator Arm by Electro-Myographic (EMG) Signals

Présentée par :

HAMZI Maroua

Soutenue publiquement le : 05 /02/ 2026

Devant les membres de Jury :

Dr MECHGOUG Raihane	**Professeur**	**Président**	**Université de Biskra**
Dr BOUMEHRAZ Mohamed	**Professeur**	**Rapporteur**	**Université de Biskra**
Dr MESSAOUDI Abdelhamid	**MCA**	**Examinateur**	**Université de Batna**
Dr CHERROUN Lakhmissi	**Professeur**	**Examinateur**	**Université de Djelfa**

Acknowledgements

First of all, I wish to express my sincere gratitude to my teacher and my advisor, Mr. BOUMEHRAZ Mohamed, Professor of University Mohammed Khider Biskra. I am highly indebted and appreciated him for giving me the chance, advices, support, and encouragement throughout the research period.

I would like to thank my jury members, namely Mr. MESSAOUDI Abdelhamid, Professor of University Mohammed Khider Biskra, Mrs. MECHGOUG Raihane, Professor of University Mohammed Khider Biskra and Mr. CHERROUN Lekhmissi, Professor of University Ziane Achour Djelfa. Their time and energy are gratefully acknowledged.

I want to appreciate very much for their detailed reviews and insightful comments. Moreover, I would especially like to thank all the Electrical Engineering department staff, for their professional treatment of me as a colleague.

I would thank my family for their patience and encouragement during my study.

I would like to thank all my colleagues and friends whose company and encouragement helped me a lot to work hard.

Last, but not the least, I thank ALLAH, for giving me the strength during the course of this research

To my family,

Abstract

Electromyography (EMG) is the record of electrical activity generated by skeletal muscles, providing information on the muscle function and movement. Several signal analysis methods have been developed in the time and frequency domains for use in different engineering applications such as myoelectric control of a prosthesis and movement analysis, mainly to overcome the complexity of EMG signals. The present thesis relies on a Myoware muscle sensor and MPU6050 board to acquire EMG signals from ten healthy volunteers in different forearm positions. Root mean square (RMS), standard deviation (STD), and mean absolute value (MAV) are calculated from each EMG signal and selected as representative features for an LDA and ANFIS classifiers to estimate the forearm flexion angles for the control of a manipulater arm purpose by developing MATLAB tools. Accordingly, this study aims to compare the effectiveness of features calculated from the EMG signal and those calculated from its wavelet decomposition. The experiment's results demonstrate the proposed method's efficiecy in estimating forearm angles of flexion using only one channel of EMG signal for four gesture classes.

Keywords: Myoware muscle sensor, linear discriminant analysis (LDA), wavelet transform, ANFIS, feature extraction.

Résumé

L'électromyographie (EMG) est l'enregistrement de l'activité électrique générée par les muscles squelettiques, fournissant des informations sur la fonction musculaire et le mouvement. Plusieurs méthodes d'analyse de signaux ont été développées dans les domaines temporel et fréquentiel pour être utilisées dans différentes applications d'ingénierie telles que le contrôle myoélectrique d'une prothèse et l'analyse du mouvement, principalement pour surmonter la complexité des signaux EMG. La présente thèse s'appuie sur un capteur musculaire Myoware et une carte MPU6050 pour acquérir les signaux EMG de dix volontaires sains dans différentes positions de l'avant-bras. La racine carrée moyenne (RMS), l'écart type (STD) et la valeur absolue moyenne (MAV) sont calculés à partir de chaque signal EMG et sélectionnés comme caractéristiques représentatives pour un classificateur LDA et ANFIS afin d'estimer les angles de flexion de l'avant-bras pour le contrôle d'un bras manipulateur en développant des outils MATLAB. En conséquence, cette étude vise à comparer l'efficacité des caractéristiques calculées à partir du signal EMG et celles calculées à partir de sa décomposition en ondelettes. Les résultats de l'expérience démontrent l'efficacité de la méthode proposée pour estimer les angles de flexion de l'avant-bras en utilisant un seul canal de signal EMG pour quatre classes de gestes.

Mots clés : Capteur musculaire Myoware, Analyse discriminante linéaire (LDA), transformation en ondelettes, mouvements de <l'avant-bras, extraction de caractéristiques

الملخص

تخطيط كهربائية العضلة (EMG) هو سجل النشاط الكهربائي الناتج عن العضلات الهيكلية، مما يوفر معلومات عن وظيفة العضلات وحركتها. تم تطوير العديد من طرق تحليل الإشارات في مجالات الوقت والتردد لاستخدامها في تطبيقات هندسية مختلفة مثل التحكم الكهربائي العضلي لليد الاصطناعية وتحليل الحركة، وذلك بشكل أساسي للتغلب على تعقيد إشارات EMG. تعتمد الأطروحة الحالية على مستشعر العضلات Myoware ولوحة MPU6050 للحصول على إشارات EMG من عشرة متطوعين أصحاء في أوضاع مختلفة للساعد. يتم حساب الجذر التربيعي المتوسط (RMS)، والانحراف المعياري (STD)، ومتوسط القيمة المطلقة (MAV) من كل إشارة EMG ويتم اختيارها كميزات تمثيلية لمصنفات LDA وANFIS لتقدير زوايا انثناء الساعد للتحكم في الذراع من خلال تطوير أدوات MATLAB. وبناء على ذلك، تهدف هذه الدراسة إلى مقارنة فعالية الميزات المحسوبة من إشارة EMG وتلك المحسوبة من تحلل المويجات. توضح نتائج التجربة كفاءة الطريقة المقترحة في تقدير زوايا انثناء الساعد باستخدام قناة واحدة فقط من إشارة EMG لأربع فئات من الإيماءات.

الكلمات المفتاحية :مستشعر العضلات Myoware، تحليل التمييز الخطي (LDA)، تحويل المويجات، ANFIS، استخلاص الميزات

Abbreviations

sEMG	Surface Electromyography Technique
LDA	Linear Discriminant Analysis
ANNs	Artificial Neural Networks
SVM	Support Vector Machines
MUAP	Motor Unit Action Potential
SENIAM	Surface EMG for non-invasive muscle evaluation
MAV	Mean Absolute Value
RMS	Root Mean Square
WAMP	Willison Amplitude
WL	Waveform Length
VAR	Variance
SM	Spectral Moments
FL	Fuzzy logicWT: Wavelet Transform
DWT	Discret Wavelet Transform
VMD	Variationnal Mode Decomposition
EMD	Empirical Mode Decomposition
SSI	Simple Square Integral
PKF	Peak Frequency
ZC	Zero crossing
IEMG	Integrated EMG
MNF	Mean Frequency
MDF	Median Frequency
MNP	Mean Power
TTP	Total Power

Journal Papers:

- HAMZI M., BOUMEHRAZ M., HASSANI R., "***Flexion Angle Estimation from Single Channel Forearm EMG Signals using Effective Features***", in *Electrotehnica, Electronica, Automatica (EEA)*, 2023, vol. 71, no. 3, pp. 53-60, ISSN 2392-828X.

- HAMZI Maroua, BOUMEHRAZ Mohamed, HASSANI Rafia, ***"Forearm EMG signals classification using and adaptive neuro-fuzzy inference system***", Electrotehnică, Electronică, Automatică (EEA), 2025, vol. 73, no. 3, pp. 152-158, ISSN 1582-5175.

- Hassani, R., Boumehraz, M., Hamzi, M., & Habba,Z. (2018). "***Gyro- Accelerometer based Control of an Intelligent Wheelchai***r", *Journal of Applied Engineering Science & Technology*, 4(1), 101-107.

- Hassani, R., Boumehraz, &M., Hamzi, M., "***Implementation of Wheelchair Controller using mouth and tongue gesture****",* Accepted in *IJEECS* Indonesian *Journal of Electrical Engineering and Computer Science.*

Communications:

- Hassani, R., Boumehraz, M., & Hamzi, M. (2018). "Head Gesture Based Wheelchair Control", *Second International Conference on Electrical Engineering ICEEB'18*, Biskra, Algeria.

- Hamzi, M., Boumehraz, M., & Hassani, R. (2018). "Hand Gesture Based Wheelchair Control", *Second International Conference on Electrical Engineering ICEEB'18*, Biskra, Algeria.

CONTENTS

LIST OF FIGURES

LIST OF TABLES

Introduction:

The surface electromyography technique (sEMG) is a non-invasive method primarily employed to assess the electrical signals generated by contracting muscles. The contractions are recorded graphically with an EMG sensor [1], [2]. It is frequently utilized due to its non-invasive nature and ease of acquisition. A single-channel EMG is sufficient for identifying diverse upper-limb muscle activations across multiple applications, including prosthetic hand control, rehabilitative electric wheelchairs, robotics, and human-computer interfaces [3].

EMG signals are influenced by a number of elements, including the structure and physiology of the muscles, as well as some sources of noise. The electromagnetic noise, motion artifacts, and intrinsic noise are the three types of noise that are most frequently found in the electromyographic (EMG) signal.

The conditioning circuitry of the EMG acquisition system influences the quality of the EMG signal. Furthermore, the device must be user-friendly, cost-effective, and sufficiently compact to fit within the socket of a prosthetic hand [4].

Contemporary EMG systems equipped with numerous characteristics provide superior EMG signal acquisition. The amplitude of a raw EMG signal obtained from the forearm muscle often falls within the 0–10 mVpp (peak-to-peak) range, whereas the frequency spectrum spans from 0–1000 Hz, with critical information predominantly located between 10 and 350 Hz [5].

Because EMG signals are complicated and extremely nonlinear, connecting the measured signal to the motion command may be difficult. As a result, the majority of studies relied on multichannel EMG, which improves motion classification efficiency.

Although the classification accuracy is improved using an EMG multichannel system, it becomes challenging to manage a big data set of characteristics when the number of channels reaches four.

While a multichannel EMG system offers benefits for classification, it also introduces complexity and clutter to the overall system. Therefore, the single-channel system method is employed to address the constraints of multichannel sEMG-based systems [6].

The forearm is seen an appropriate site for the implantation of the EMG signal acquisition system, owing to the diverse range of motions generated by the arm, irrespective of the amputated user. EMG signals can be collected from the muscles located in the stump where the prosthetic device will be affixed [7].

Following data gathering, the extraction of precise features is crucial, as the efficacy of a method for categorizing patterns is intricately linked to the judicious selection of features that reflect the EMG signal [8].

Time domain features are extensively utilized, including root mean square (RMS), variance of EMG (VAR), mean absolute value (MAV), zero crossing (ZC), simple square integral (SSI), Willison amplitude (WAMP), waveform length (WL), and integrated EMG (IEMG) [9].

At various time intervals, an EMG signal encompasses distinct frequencies; the fast Fourier transform (FFT) and the short-term Fourier transform (STFT) are two prominent techniques for determining the frequency spectrum of an EMG signal.

The amplitude of each frequency can be ascertained using the frequency spectrum. Additionally, characteristics such as peak frequencies, median frequency (MDF), and mean frequency (MNF) can be derived from the signal [10], [11].

These approaches necessitate a stationary signal to extract significant features; however, the EMG is non-stationary [12].

In the joint time-frequency domain, features can also be expressed, which allows for the physical observation of the signal by utilizing the frequency and time domain features of the EMG signal [9].

The Wavelet Transform (WT) produces a time-frequency representation. The latter computes the convolution of the signal using a particular mother wavelet at varying scales and

times [13]. The representation encompasses many resolution levels, and the features acquired are substantial due to the computation including various wavelets, leading to enhanced movement recognition.

Upon choosing a suitable wavelet shape, the resulting WT delivers the most precise depiction of energy throughout the movement in the time-frequency domain [7], [14].

Recent studies confirm the advantages of employing wavelet transform for the analysis of EMG signals. Chowdhury in [15] examines the favorable outcomes achieved through the application of Daubechie's functions by reviewing various studies related to the wavelet transform.

Following the feature extraction process, a variety of classifiers have been employed to classify or predict human arm motion, including fuzzy systems, fuzzy-genetic approaches, neuro-fuzzy models, artificial neural networks (ANNs), and support vector machines (SVMs). All these models yield commendable outcomes. Nonetheless, the chosen classifier was linear discriminant analysis (LDA) due to its effectiveness, straightforwardness, and rapid classification capabilities [16].

In this study, the goal was to find ways to group EMG signals from certain hand movements that were recorded by a MyoWare muscle sensor. The effectiveness of various time domain and frequency domain features on identifying motions and figuring out how well the chosen classifier worked was compared by looking at the effects of extracted features and feature combinations on classification accuracy.

The subsequent sections of this thesis are structured as follows.

Chapter 1: This chapter offers a succinct introduction to the origins of EMG signals and the fundamental requirements for their acquisition, accompanied by a review of electrode types and sources of noise. The chapter's end provides a detailed account of electrode placement on the muscle for EMG signal recording.

Chapter 2: This chapter provides a detailed analysis of the properties of EMG signals. We first introduce time-domain features that enhance the pattern identification process. Subsequently, an analysis of EMG signal characteristics in the frequency domain is generally performed to assess muscle movements. Ultimately, we offer an overview of the essential principles of time-frequency domain features to attain a more accurate physical representation of the signal.

Chapter 3: This chapter discusses the fundamental design and applications of widely used classifiers, including ANN, FL, SVM, and LDA, for the regulation of myoelectric prosthetics.

Chapter 4: This chapter presents the results that were obtained, together with the dataset and the approach that we have provided for classifying the EMG signal and arm manipulator control.

Chapter 5: This chapter presents the simulation and results of a (2-DOF) arm manipulator control and validate the theoretical kinematic equations through simulation and graphical results.

CHAPTER 1

Introduction to EMG Technique

1.1. Introduction

The human body relies on the nervous system to carry out essential tasks, with the brain being key to controlling both voluntary and involuntary actions. The brain is constantly active, managing a complex network of nerve activity. This process involves a group of neurons that work together after being excited, which leads to the movement of ions across their membranes.

The electromyography (EMG) signal is an electrical indication of neuromuscular actuation associated with contracting muscles. It's a very complicated signal that is affected by the structure and function of muscles, the way the peripheral sensory system is controlled, and the features of the equipment used to find and track it. The majority of the links between the EMG signal and the features of a rapidly contracting muscle have emerged by chance. The lack of a suitable representation of the EMG signal is likely the most significant single aspect impeding the development of EMG into an accurate science.

The following is the outline of this chapter: Initially, we provide a brief overview of the source of the EMG signal, and subsequently, we elucidate the critical conditions for its acquisition. The strategies discussed at the conclusion of the chapter are quite comprehensive when it comes to the placement of electrodes.

1.2. EMG signal source

Research on EMG signal-based control systems is ongoing for HMI applications, especially in rehabilitation. Electromyography (EMG) is a methodological approach for quantifying and documenting a sequence of electrical impulses generated by skeletal muscles [17]. EMG signals result from physiological alterations in the state of muscle fiber membranes. The modulation of muscle fiber excitability by the brain is a crucial aspect of muscular physiology. Moreover, EMG signals originate from action potentials at the muscle fiber membrane resulting from depolarization and repolarization [18].

Figure1.1 illustrates this phenomenon through a semi-permeable membrane model that delineates the electrical properties of the sarcolemna (the cell membrane of skeletal muscle).

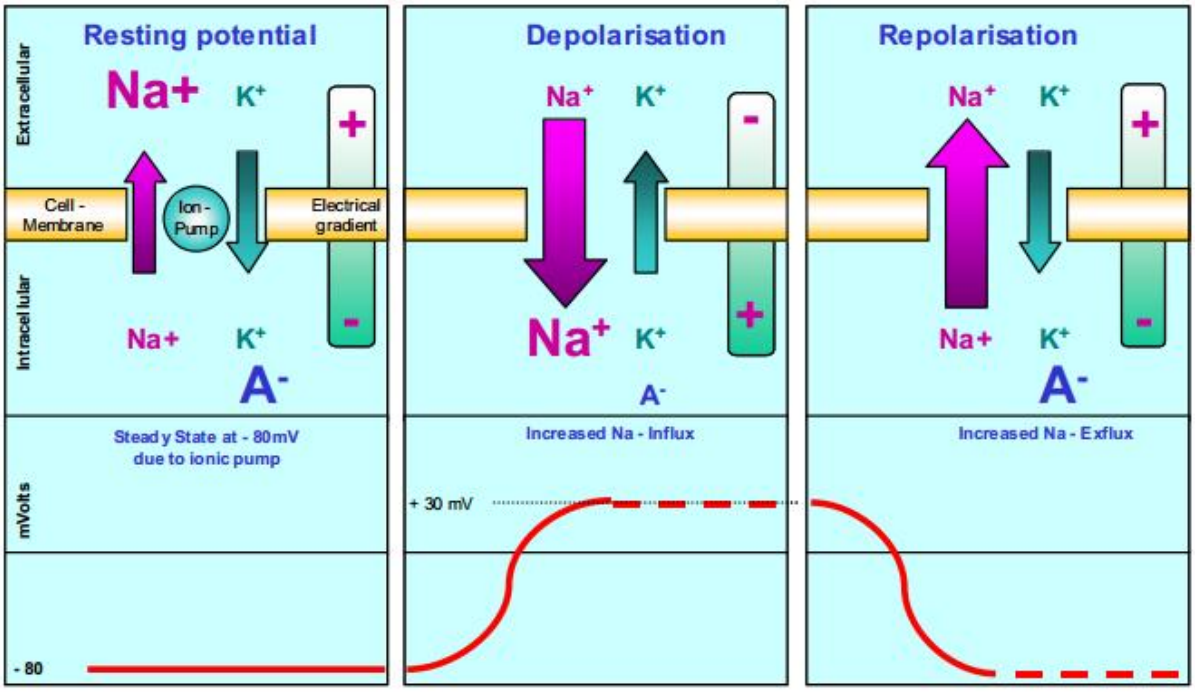

Figure 1.1: A schematic representation of the repolarization/depolarization cycle in excitable membranes.

Figure 1.1 illustrates that when a muscle cell is in a relaxed state, the resting potential of the muscle fiber membrane is approximately -80 to -90 mV. This is due to the ionic equilibrium

between the intracellular and extracellular environments of the muscle cells. Surface EMG signals have amplitudes that range from μV to mV, depending on the type of muscle and the conditions of the observation [19].

The difference in potential is kept up by physiological mechanisms (ion pumps), which causes a negative charge inside the cell compared to the outside. When the central nervous system or a reflex turns on an alpha-motor anterior horn cell, it sends excitement through the motor nerve. Subsequent to the discharge of neurotransmitters at the motor endplates, an endplate potential develops in the muscle fiber innervated by the respective motor unit. The diffusion characteristics of the muscle fiber membrane are temporarily modified, allowing Na+ ions to enter. This induces membrane depolarization, which is promptly rectified by an ionic exchange in the reverse direction inside the active ion pump mechanism. This procedure is also referred to as repolarization [20].

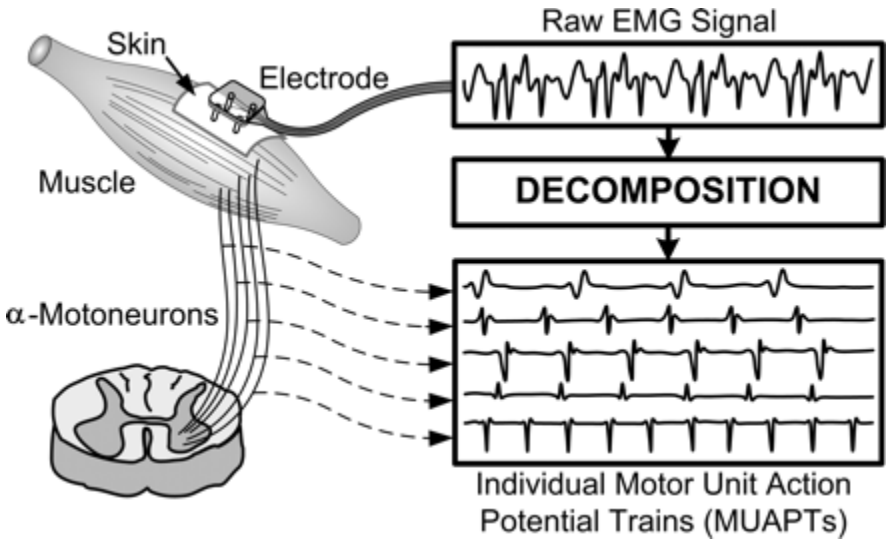

Figure 1.2: Decomposition of a raw EMG signal results from individual TPAUMs [21].

The motor unit action potential (MUAP) is the sum of the action potentials of all the muscle fibers in a single motor unit [22]. Non-invasive or invasive techniques can be employed to detect the MUAP referenced in figure 1.2.

- An non-invasive method involves putting electrodes or sensors directly on the skin in order to record and pick up electromyographic (EMG) signals.

- An invasive method, on the other hand, involves inserting a needle or wire electrode into muscle tissue.

It is important to note that the non-invasive method is recommended for monitoring EMG signals because it does not cause any discomfort and has a low risk of infection for amputees [23-26].

The amplitude of surface EMG signals ranges from 0 to 10 mV, with a frequency range of 10 to 500 Hz. EMG is used to quantify the electrical signal that is linked to muscle contraction. Compression of the muscles may be either intentional or automatic. The EMG action of voluntary muscle disengagement is associated with pressure. The practical unit of muscle compression is the engine unit, which is exemplified by a single alpha engine neuron and all the filaments it exhausts. When the nerve that supplies this muscle fiber reaches a depolarization limit, it contracts due to the activity possibilities (drive). The potential is quantified as a voltage, and an electromagnetic field is produced by the depolarization. The depolarization that propagates throughout the muscle membrane is referred to as a muscle activity potential. Engine unit activity potential is the sum of the individual muscle activity potentials for all the filaments in a single engine unit over time and space. It is the mathematical sum of all the possible engine unit activities that can happen in the pick-up area of the current terminal. The pick-up zone of a cathode frequently contains multiple engine units as a result of the intermixing of muscle filaments from various engine units throughout the entire muscle [20]. 20–50 engine units may be present in filaments that are situated in any region of the muscle. There are two main types of EMG: clinical (also known as indicative EMG) and kinesiological.

- ✓ The engine unit's activity potential for span and abundance is examined through symptomatic EMG, which is typically performed by physiatrists and neurologists. These are frequently employed to facilitate the analysis of neuromuscular pathology. Additionally, they are capable of evaluating spontaneous muscle releases and restricting the action of a single engine unit.

- ✓ Kinesiological EMG is the most frequently employed variety in developmental dissection literature. This type of EMG looks at the connection between substantial capacity and body fragment growth, as well as the timing of muscle activation in relation to these changes. Additionally, a variety of studies are conducted to examine the composition and energy generation of the muscles [27].

1.3. Electrode Types

There are two types of surface electrodes that are regularly used:

• Dry electrodes make direct touch with the skin.

• Gelled electrodes use an electrolytic gel to form a chemical interaction between the skin and the electrode's metallic component.

1.3.1. Dry Electrodes

Dry electrodes are primarily employed in applications where the geometry or size of the electrodes does not allow gel.

Dry electrodes include array electrodes and bar electrodes. Because of the high electrode-to-skin impedance associated with dry electrodes, the pre-amplifier circuitry is frequently located at the electrode site. Dry electrodes (>20g) are much heavier than gelled electrodes (<1g). In comparison to gelled electrodes, the additional inertial mass makes it more difficult to maintain electrode fixation [28].

Figure 1.3: Dry Electrodes.

1.3.2. Gelled Electrodes

Gelled electrodes use an electrolytic gel to form a chemical interaction between the skin and the electrode's metallic component. Chemical reactions, both oxidative and reductive, occur in the contact region between the metal surface and the gel.

Figure 1.4: Gelled Electrodes.

The most frequent compound for the metallic component of gelled electrodes is silver-silver chloride (Ag-AgCl). The AgCl layer permits current from the muscle to flow more readily across the interface between the electrolyte and the electrode. This introduces less electrical noise into the measurement as compared to equivalent metallic electrodes (e.g., Ag). Because of this, Ag-AgCl electrodes are used in more than 80% of surface EMG applications [13].

Gelled electrodes can be disposable or reusable. Disposable electrodes are the most frequent since they are so light. Disposable electrodes are available in a variety of forms and sizes, and the materials used to make the patch as well as the shape of the conductive gel vary by manufacturer. With careful application, disposable electrodes limit the danger of electrode displacement, even during fast movement [29].

1.4. SENIAM's Recommendations for Bipolar EMG Electrodes

The SENIAM (surface EMG for non-invasive muscle evaluation) initiative was organized as a European concerted action, with funding from the European Community's Biomed 2 program (1996-99). The initiative aimed to integrate basic and applied research on surface EMG (sEMG) at the European level [30].

The SENIAM project has provided suggestions for the development of bipolar electromyography (EMG) electrodes (sensors), which include the following: electrode form; electrode size; inter-electrode distance; electrode material; electrode structure.

1.4.1. Electrode Form

The electrode form is defined as the shape of the conducting region. Electrodes might be circular, square, or bar-shaped. The practical implication is that the surface area of each electrode site (i.e., bipolar) should be the same, resulting in equal input impedances and limited common mode disturbance. SENIAM identified no obvious and objective criterion for recommending electrode shape.

1.4.2. Electrode Size

• The electrode size is defined as the size of the surface of a conductive area of a sEMG electrode. SENIAM recommends that the “size of electrodes in the direction of the muscle fibers is maximum 10mm.

• It is believed that as the size perpendicular to the muscle fibers (bar electrodes) rises, so will the view of the electrodes. There is currently no quantifiable evidence available on the magnitude of this effect on sEMG features.

• raising the size in the direction of the muscle fibers has been demonstrated to have an integrative effect on the sEMG signal, raising the observed amplitude and decreasing the high frequency contents.

• The European inventory revealed that round electrodes with a circular diameter of 10mm are the most popular.

• For bipolar sensors, the electrodes should be large enough to record a reasonable pool of motor units while being small enough to avoid crosstalk from other muscles.

1.4.3. Inter-Electrode Distance

• The inter-electrode distance is the center-to-center distance between electrodes' conducting regions.

• An important aspect that is discussed in the research literature is the impact that the distance between the electrodes has on the pick-up area and crosstalk.

• SENIAM suggests that the bipolar sEMG electrodes be applied in a 20mm-diameter circle around the recommended sensor location.

• When applying bipolar electrodes to muscles that are comparatively small, the inter-electrode distance should not exceed ¼ of the muscle fiber length. By doing so, it is possible to prevent the occurrence of unstable recordings that are caused by tendon and motor end-plate effects.

1.4.4. Electrode Material

SENIAM advises the use of pre-gelled Ag/AgCl electrodes.

• The electrode material that forms the contact layer with the skin must exhibit a stable behavior over time, a low electrode-skin impedance, and a good electrode skin contact (i.e., with regard to impedance and chemical reactions at the skin interface).

• An inventory has shown that different types of materials are used: Ag/AgCl (silver/silver-chloride), AgCl (silver-chloride), Ag, etc.

The majority of electrodes are combined with electrode gel.

• Electrode gel and paste are employed to decrease the impedance between the electrode and the skin.

• The performance of disposable and reusable electrodes is comparable; however, the risk of improper and inconsistent measurement characteristics is elevated with reusable electrodes due to their altered impedance.

1.4.5. Electrode Structure

• Defined as the (mechanical) structure that integrates the electrodes, cables, and (if applicable) the pre-amplifier.

• SENIAM advises the use of a construction composed of lightweight materials and a fixed inter-electrode distance.

• In order to prevent the formation of pulling artifacts, cables must be secured with adhesive or an elastic band. If the sensor construction causes an excessive amount of (movement) artifact due to its inertia during fast dynamic contractions, SENIAM suggests that the inter electrode distance be fixed using (double-sided) tape or rings.

• It is anticipated that the sEMG characteristics will not be immediately influenced by the construction (and its mass). However, there are some potential indirect effects that may disrupt or interfere with the recorded sEMG pattern.

• The amplitude, shape, and width of the action potentials will be modulated, resulting in an interference pattern that is altered in terms of its amplitude and frequency characteristics, if the sensor's construction allows for a variation in the inter-electrode distance during muscle contraction.

• The potential for movement artifacts exists if the sensor's construction allows for the movement of electrodes and cables, which may be caused by the inertia of the construction or the dragging of cables.

1.5. Noise Sources

EMG signals are influenced by a variety of factors, such as noise sources and muscle anatomy and physiology.

The quality of the EMG signal is determined by the conditioning circuitry of the EMG acquisition system. Additionally, the device must be compact enough to accommodate within the socket of a prosthetic hand, inexpensive, and user-friendly [31].

Because EMG signals are complicated and extremely nonlinear, connecting the measured signal to the motion command may be difficult. As a result, the majority of studies relied on multichannel EMG, which improves motion classification efficiency.

Although the classification accuracy is improved using an EMG multichannel system, it becomes challenging to manage a big data set of characteristics when the number of channels reaches four.

Classification benefits from an EMG multichannel system, but the system becomes cluttered and complicated as a result. Since multichannel sEMG-based systems have many limitations, the single-channel system technique is employed to circumvent them [32].

When it comes to the detection and recording of electromyographic (EMG) signals, there are two primary concerns that have an impact on the fidelity of the signals:

- Signal-to-noise ratio
- Noise signal

This issue analyzes the ratio of energy present in EMG signals compared to that in noise signals. Noise is typically defined as electrical signals that do not constitute the desired EMG signal [33].

1.6. Types of noise

1.6.1. Ambient Noise

Ambient noise is produced by electromagnetic devices, including computers, force plates, and power lines. Any device connected to a wall A/C (Alternating Current) outlet produces ambient noise. The noise exhibits a broad spectrum of frequency components, with the predominant frequencies being 50Hz or 60Hz, which align with the frequency of the alternating current power supply (i.e., wall outlet).

1.6.2. Transducer Noise

Transducer noise originates at the electrode-skin interface. Electrodes convert ionic currents produced in muscles into electronic currents, which can be processed by electronic circuits and stored as voltage potentials in either analog or digital formats.

Two types of noise sources arise from the transduction process from ionic to electronic form:

• D/C (Direct Current) Voltage Potential: arises from variations in impedance between the skin and the electrode sensor, as well as from oxidative and reductive chemical reactions occurring in the contact area between the electrode and the conductive [28].
• A/C (Alternating Current) Voltage Potential: produced by variations in impedance between the conductive transducer and the skin. Utilizing Ag-AgCl electrodes is an effective approach to reduce impedance effects. This electrode comprises a silver metal surface coated with a thin layer of silver chloride [29].

Optimization of the signal-to-noise ratio is the primary goal of EMG measurements. The noise level in the EMG signal has been diminished as a result of technological advancements. The bipolar recording technique was a substantial advancement when it was introduced. A differential amplifier is utilized in conjunction with bipolar electrode configurations to reduce signals that are shared by both electrodes. In the process of differential amplification, the potential at one electrode is subtracted from that at another, and the resulting difference is subsequently amplified.

Correlated signals prevalent at both locations, including those from power sources and electromagnetic equipment, as well as EMG signals from remote muscles, are attenuated. Furthermore, the D/C components, including the over-potential produced at the electrode-skin interface, will be detected with comparable amplitude (as detailed below) and will consequently be attenuated.

In contrast, signals from muscle tissue in close proximity to the electrodes will be amplified and are not correlated. The emergence of bipolar recordings with differential pre-amplification has facilitated the recording of the complete EMG bandwidth and increased the spatial resolution (i.e., the size of the recording area). This also results in an increase in the signal-to-noise ratio.

The quality of the electrode-skin contact significantly influences the differential amplification process in bipolar EMG studies. The contact between the electrode and skin is quantitatively determined by the resistance of the skin and underlying tissues, as well as the capacitance of the electrodes. It is usually referred to as electrode-skin impedance.

1.7. The Significance of Skin-Electrode Impedance

The reliability of EMG measurements is contingent upon the consistency of impedance. The significance of measuring EMG with low electrode-skin impedance has been diminished by the high input impedance of modern pre-amplifier designs. Although the absolute level of muscle impedance is not a critical factor, the signal-to-noise ratio of the measured EMG signal is significantly influenced by the stability of impedance over time and the balance of impedance between electrode sites , both in terms of spatial resolution and noise levels [34].
The impedance equilibrium between electrode sites is crucial for the reduction of noise components. It is not necessary for the impedances at each site to be perfectly balanced; however, they should be relatively similar. Among other factors, the impedance balance level is somewhat arbitrary and is contingent upon the properties of the differential pre-amplifier in use.
The impedance indicates the amount of energy present in the electrical signal at each electrode site. This information provides insight into the electrode's perception of the muscle and its surroundings. The impedance between electrode sites affects the signal amplitude that undergoes differential amplification. Common signal components are eliminated solely by differential amplification. For instance, differential amplification will retain a portion of the noise in the signal if the energy of power-line noise differs [28]. In the same vein, the voltage potential of the D/C will differ, and a portion of it will not be cancelled. The preamplifier may become unstable, inaccurate, or saturated after being amplified if the remaining D/C component is not sufficiently cleaned of D/C noise.

The general rule is that the signal-to-noise ratio increases as the electrode-skin impedance between electrodes sites becomes more evenly distributed, resulting in a lower noise level. It is challenging to predict or quantify the extent to which imbalanced impedance affects the properties of the EMG signal due to its complexity. This statement alone is enough to say that achieving a similar equilibrium in impedance is the best way to make EMG measurements more reliable.

Impedance must also be consistent throughout the measurement. The signal-to-noise ratio and the EMG signal's spatial resolution will drift if the impedance drifts during measurement for similar reasons. New evidence suggests that electrode-skin impedance considerably affects

EMG signal power. EMG frequency components below 100 Hz had higher energy when the electrode-skin impedance was low (<10 kOhm) compared to high (>100 kOhm).

On the other hand, experiments with low electrode-skin impedance produced a lower signal energy level for EMG signal frequency components between 100 and 150 Hz compared to those with high impedance. Similar results from other studies back up what [20] found, which suggests that changes in electrode-skin impedance can change spatial resolution (i.e., the electrical view of the muscle). Consequently, it is crucial that the impedance remain stable during the measuring session [35, 36].

1.7.1. Skin Preparation

A D/C voltage potential is generated at the electrode–skin interface, primarily due to a sustantial increase in impedance from the outermost layer of skin, which includes decaying skin material and oil secretions. The D/C potential, which is universally present in all electrodes, can be reduced through appropriate skin preparation. Indeed, the quality of contact is typically diminished by a minimum of ten times with appropriate preparation [37].

1.7.2. Cross Talk

It's important to know that bipolar sEMG does not always show the electrical activity of just one muscle right under the recording electrodes. Smaller muscles might not be detected properly by the probes, which can lead to signals from other nearby muscles mixing with the signals from the muscle you want to measure. Signals from muscles near the probe will mainly affect the recorded sEMG signal, while signals from farther muscles may mix in and create noise.

The distance for accurate electrode measurement is the area around the electrode where the signal is stronger than the background noise. As the distance from the recording electrode grows, the bipolar sEMG signal's amplitude decreases at a very fast rate [38]. This happens because muscle fibers, fat under the skin, and skin itself are not the same in all directions. They act like a filter that allows lower frequency signals to pass through, and as the distance between the muscle fibers and the electrode grows, this filtering effect becomes stronger. This means that as electrical sources get farther away, it becomes harder to measure the signals

they produce. Also, the signals from sEMG will have lower frequencies as the sources get more distant [30]

Crosstalk can be avoided by choosing the appropriate size of the electrodes conductive area and the appropriate inter-electrode distance. Decreasing the size of the conductive area reduces the effective sEMG measurement distance (i.e. depth). Similarly, decreasing the inter-electrode distance decreases the effective recording distance and shifts the EMG bandwidth to higher frequencies.

1.8. Electrodes Localization

The EMG signal reflects the electrical activity in a muscle or muscles during contraction. The electrical perspective is significantly influenced by the position of the electrode next to the targeted muscle. The placement of the electrodes affects the electrical representation of a muscle. For this reason, it is important that the electrodes are always placed in the same way for EMG measurements, both between people and between recording sessions [27].

The sensor location is specified as the position of the two bipolar sites situated above a muscle in reference to a line connecting two anatomical landmarks. The objective of sensor placement is to identify a position that yields a reliable and robust surface EMG signal.

Two primary methodologies exist for the installation of electrodes. The electrode can be positioned longitudinally along the muscle's long axis or transversely, perpendicular to it, from the skin surface.

• The bipolar electrode configuration should be halfway between the distal motor end plate (muscle midline) and the distal tendon. The sensor should not cover the innervations zone or tendon throughout motion.

• Transverse: Put the bipolar electrode on the muscle so each sensor is away from the muscle recording area of interest. This can include huge muscle compartments and nearby muscles under the electrode. This means the line between the electrode sensor centers is usually parallel to the muscle's long axis.

Example of electrodes placement on biceps, deltoid, triceps, tibialis anterior, and quadriceps muscles are illustrated in (Figures1.5, 1.6, 1.7, 1.8, and 1.9).

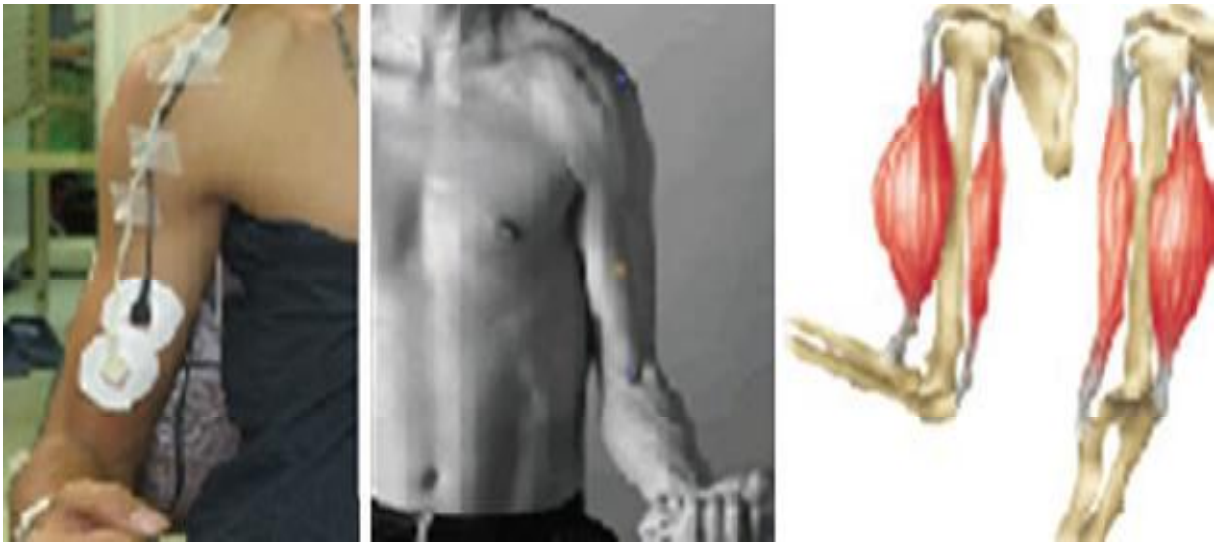

Figure 1.5: Deltoid anatomy and electrode placement.

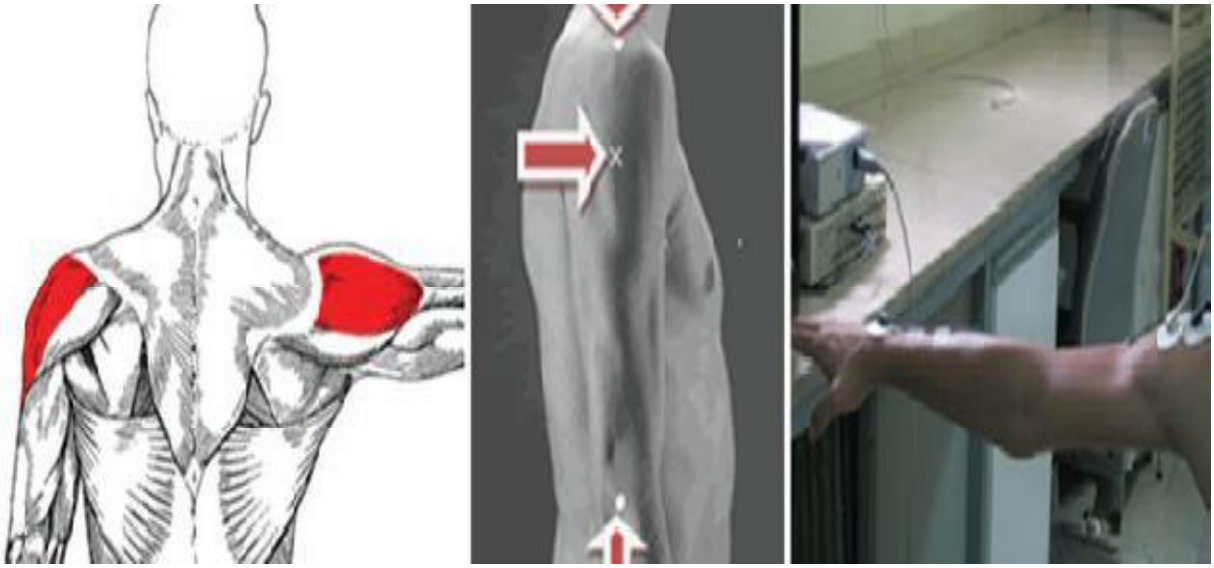

Figure 1.6: Deltoid anatomy and electrode placement.

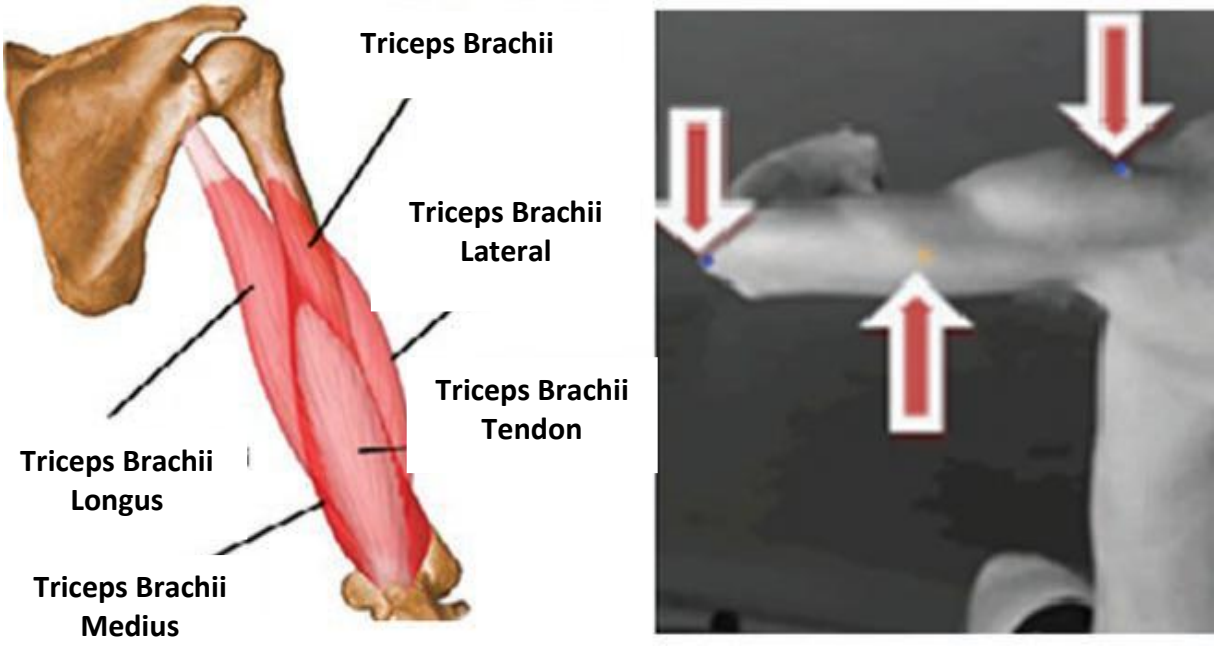

Figure 1.7: Triceps anatomy and electrode placement.

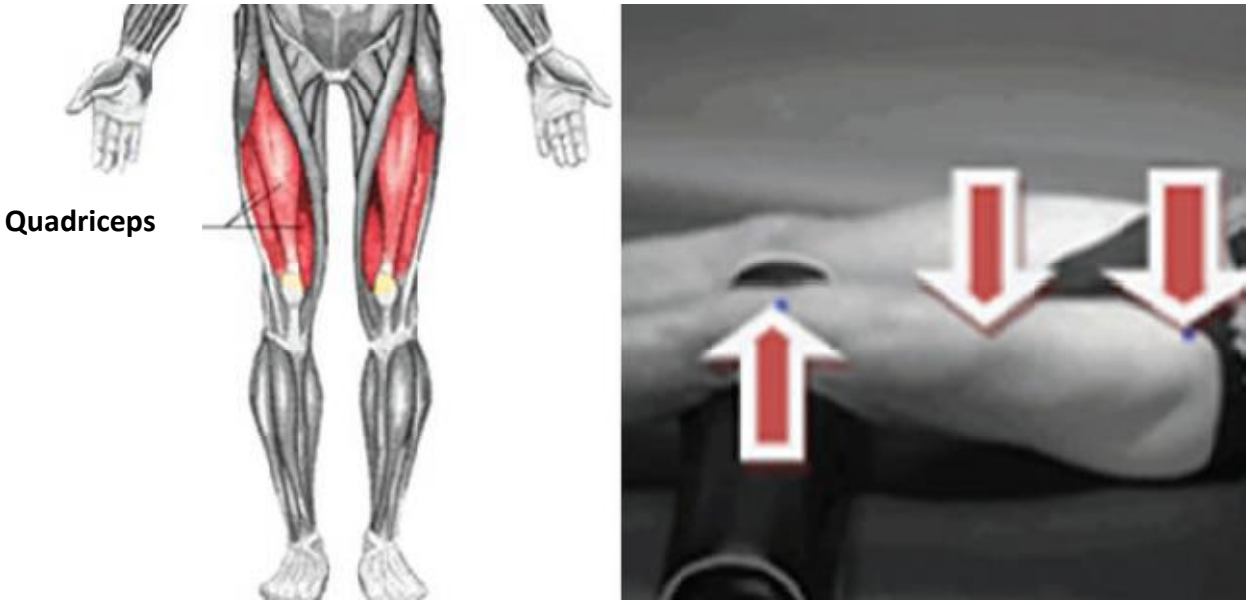

Figure 1.8: Quadriceps anatomy and electrode placement.

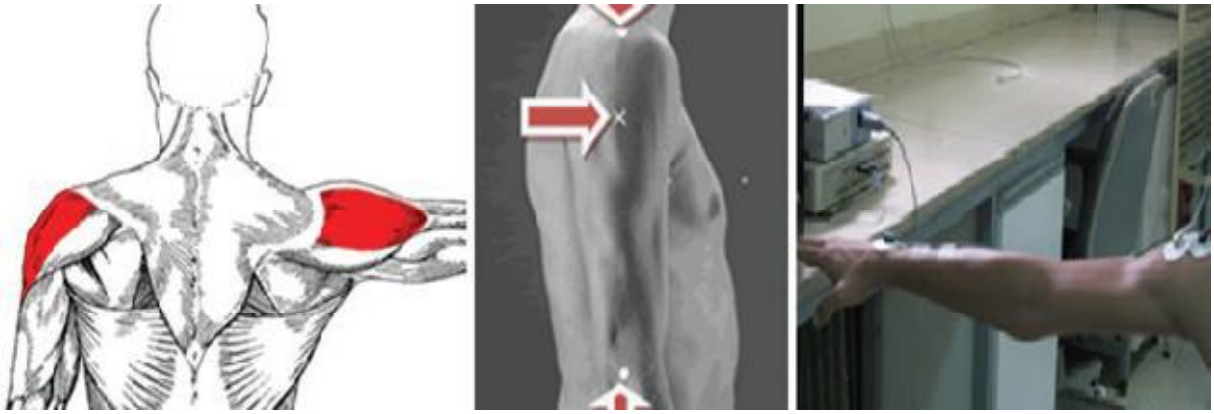

Figure 1.9: Tibialis anterior anatomy and electrode placement.

1.9. Conclusion:

This chapter provides a concise introduction to the source of EMG signals and the essential needs for their capture, followed by an overview of electrode types and noise sources. The electrode placement on the muscle for EMG signal recording is detailed at the chapter's conclusion.

Subsequent chapters outline the feature extraction and classification techniques employed in our study to analyze specific motions of the human forearm.

CHAPTER 2

EMG Feature Extraction Methods

2.1. Introduction:

Feature extraction, a process for quantifying characteristics or attributes from input data, is crucial in the design of pattern recognition systems. The objective of feature extraction is to define an item for recognition by measures that exhibit high similarity across objects within the same category and significant dissimilarity among objects from different categories. Computational complexity and class discrimination are the primary variables for identifying the optimal feature set.

This chapter offers a comprehensive description of the characteristics of EMG signals. Initially, we present features articulated in the time domain that are advantageous for the pattern recognition process. Subsequently, an examination of EMG signal characteristics in the frequency (or spectral) domain is primarily conducted to analyze muscle movements. Finally, we provide an introduction to the fundamental concepts of time-frequency domain features to achieve a more precise physical representation of the signal.

2.2. EMG Signal Features

The measurement of EMG signals acquired during muscle or muscle group contractions is essential to correlate these signals with distinct movement categories.

The feature extraction method may be utilized to delineate the mathematical representation of EMG signals. An EMG signal can be depicted in two domains: frequency and time.[39]

Feature extraction is a technique employed to derive valuable information concealed within surface EMG signals while eliminating extraneous EMG components and interferences. The fundamental objective of the feature extraction phase is to utilize these features to identify an optimal set that accurately describes and characterizes EMG signals as in Figure 2.1

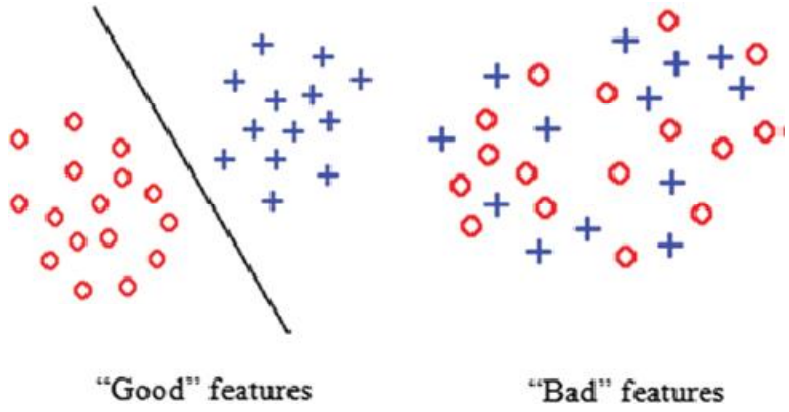

Figure 2.1: Feature extraction purpose.

2.2.1. Time Domain Features

Time domain features are advantageous for pattern recognition as they do not necessitate a transformation step. The rapid and straightforward computation of characteristics mitigates latency, a significant issue in the operation of human arm prosthesis. Researchers have presented a diverse array of time domain parameters for the classification of movement or force [40]. Let x_k represent the k_{th} EMG sample and N denote the total number of samples in each segment; the most commonly utilized time domain features are outlined as follows.

2.2.1.1. Mean Absolute Value

The mean absolute value (MAV) of an EMG signal is the average of the absolute values of sequential signal amplitudes. MAV is among the most utilized characteristics and is defined as follows:

$$MAV = \frac{1}{N}\sum_{K=1}^{N}|x_k| \qquad (2,1)$$

2.2.1.2. Root Mean Square

The Root Mean Square (RMS) feature denotes a computation of an amplitude-modulated Gaussian random process associated with constant force and non-fatiguing contraction. The mathematical representation of the RMS is expressed as,

$$RMS = \sqrt{\frac{1}{N}\sum_{k=1}^{N} x_k^2} \qquad (2,2)$$

2.2.1.3. Willison Amplitude

The Willison amplitude (WAMP) feature quantifies the frequency with which the EMG signal amplitude above a specified threshold. WAMP serves as an indicator of motor unit action potentials (MUAP) and contraction force in muscles, which can be mathematically represented as follows:

$$WAMP = \sum_{k=1}^{N}[f(|x_k - x_{k+1}|)] \qquad (2,3)$$

$$f(x) = \begin{cases} 1, if\ x \geq threshold \\ 0,\ therwise \end{cases}$$

2.2.1.4. Waveform Length (WL)

The waveform length (WL) of an EMG signal is the total length of the waveform across the time interval. The WL feature can be computed as follows:

$$WL = \sum_{k=1}^{N-1} |x_{k+1} - x_k| \qquad (2,4)$$

2.2.1.5. Variance of EMG (VAR)

The variance of EMG (VAR) denotes the second-order moment of the EMG signal and serves as a measure of power. The VAR feature can be delineated as follows:

$$VAR = \frac{1}{N-1} \sum_{k=1}^{N} x_k^2 \qquad (2,5)$$

2.2.1.6.Simple Square Integral (SSI)

The Simple Square Integral (SSI) of an EMG signal denotes the summation of the squared amplitudes of the EMG signal over a certain time interval. SSI may be articulated as,

$$SSI = \sum_{k=1}^{N} x_k^2 \qquad (2,6)$$

2.2.1.7. Zero Crossing (ZC)

The zero crossing (ZC) feature quantifies the frequency at which the amplitude of the EMG signal intersects the zero level. A threshold setting is established to mitigate voltage fluctuations or the effects of noise. The calculation of the ZC feature can be defined as follows:

$$ZC = \sum_{k=1}^{N-1} [sng(x_k \times x_{k+1}) \cap |x_k - x_{k+1}| \geq threshold] \qquad (2,7)$$

$$sng\ (x) = \begin{cases} 1, if\ x \geq threshold \\ 0, otherwise \end{cases}$$

2.2.1.8. Integrated EMG (IEMG)

Integrated EMG denotes the summation of absolute values of EMG amplitude throughout each time segment. The IEMG characteristic is utilized for clinical applications and can be articulated as follows:

$$IEMG = \sum_{k=1}^{N} |x_k| \qquad (2,8)$$

2.2.2. Frequency Domain Features

The analysis of EMG signal characteristics in the frequency (or spectral) domain primarily aims to examine muscle exhaustion and motor unit recruitment [41]. Diverse feature types have been proposed to address EMG signal behavior in the frequency domain.

While f_j ,P_j and M and M denote the frequency value at frequency bin j, the EMG power spectrum at frequency bin j, and the length of frequency bin, respectively. The following are some frequency domain properties.

2.2.2.1. Mean Frequency (MNF)

The mean frequency (MNF) is calculated by dividing the sum of the product of the EMG power spectrum and frequency by the whole sum of the spectrum intensity. The mathematical expression is presented as follows:

$$MNF = \frac{\sum_{j=1}^{M} f_j P_j}{\sum_{j=1}^{M} P_j} \qquad (2,9)$$

2.2.2.2.Median Frequency (MDF)

The median frequency (MDF) of an EMG signal is the frequency at which the spectrum is divided into two equal amplitudes. The MDF characteristic can be computed as follows:

$$\sum_{j=1}^{MDF} P_j = \frac{1}{2}\sum_{j=1}^{M} P_j \qquad (2,10)$$

2.2.2.3. Peak Frequency (PKF)

The frequency that encompasses the maximum power is referred to as the peak frequency (PKF). The PKF can be calculated as follows:

$$PKF = max(P_j) \qquad (2,11)$$

2.2.2.4. Mean Power (MNP)

The average power spectrum of EMG signals is utilized to ascertain the signal's properties. The characteristic can be articulated mathematically as,

$$MNP = \frac{1}{M}\sum_{j=1}^{M} P_j \qquad (2,11)$$

2.2.2.5. Total Power (TTP)

The aggregate of the power spectrum of the EMG signal indicates an additional characteristic, specifically the total power (TTP), which is derived as follows:

$$TTP = \sum_{j=1}^{M} P_j \qquad (2,12)$$

2.2.2.6. Spectral Moments (SM)

Spectral moments (SM) represent a significant method for feature extraction. The mathematical equations for the first (SM_1) and second (SM_2) order spectral moments are provided below, notwithstanding the possibility of calculating higher order spectral moments

$$SM_1 = \sum_{j=1}^{M} P_j f_j$$

$$SM_2 = \sum_{k=1}^{M} P_j f_j^2 \qquad (2,13)$$

Electromyography signals can also be analyzed in the joint time-frequency domain.
To get a more precise characterization of the signal in a physical context, EMG signals may be converted to a domain that include both frequency and time domain characteristics. This transition necessitates substantial computing expenses and may result in delays in the control of assistive devices. The principal characteristics of the time-frequency domain include the (WT), Wavelet Packet Transform (WPT), and Short-Time Fourier Transform [39].

2.2.3. Time-Frequency Domain Features

A greater amount of information about the signal can be extracted by combining time and frequency features in time-frequency domain representations (TFRs). Regarding pattern recognition, particularly EMG pattern recognition, TFRs have garnered significant attention .

The primary motivation for employing these representations as a feature in SEMG pattern recognition is to acquire additional information about the signal to enhance discrimination among different movements. The wavelet transform (WT) is a renowned form of these representations. Wavelet analysis, akin to the Fourier transform that decomposes a signal into sine waves of differing frequencies, is employed to decompose a signal into shifted and scaled representations of the original (or mother) wavelet [42].

2.2.3.1 Properties of Wavelets:

The characteristics of wavelets serve as a crucial reference for the construction of wavelets or the selection of appropriate wavelets for processing diverse data. Farge [43] has examined the considerations necessary for selecting the mother wavelet, including orthogonality, the nature of values (negative and real), as well as the width and form of the mother wavelet. Wavelets possess numerous fundamental qualities or criteria: vanishing moment, support length, regularity, symmetry, and orthogonality.

The orthogonal wavelet exhibits excellent time-frequency localization properties. Selesnick delineated the requisite requirements for an orthogonal wavelet system to constitute a Hilbert transform pair [44] and introduced a building procedure predicated on a delay filter in [45], [46]. Selesnick additionally noted that the requisite conditions outlined in [44] remain sufficient [31]. The vanishing instant is defined as [47]. For a wavelet with N vanishing moments, the following condition must be met:

$$\int t^{P} \Psi(t)dt = 0 \qquad (2,14)$$

where $0 \leq p < N$, $\Psi(t)$: is the wavelet function, and t is the time variable of the wavelet function. Higher vanishing moments of wavelets are necessary for the rapid calculation, denoising, and compression of signals. The greater the vanishing moment, the more wavelet coefficients are zero.

The wavelet function's support interval is the extent at which the function converges from a finite value to 0 as the time or frequency approaches infinity.

Regularity is typically employed to characterize the smoothness of a function. A specific degree of regularity (smoothness) is typically necessary for wavelet analysis to get an improved reconstruction of the signal. The wavelet function has the same regularity as the scale function, as it is derived from a linear combination of translations of the equivalent scale function. To mitigate the impact of reconstruction error on human perception during the quantization of wavelet coefficients, it is imperative to enhance the smoothness or continuous differentiability of the wavelet to the greatest extent feasible. Wavelets exhibiting adequate regularity can attain superior smoothing effects in signal or image reconstruction. Nonetheless, if the regularity is adequate, the support length will increase, resulting in higher computational costs. A strong correlation exists between vanishing moments and regularity[48].

In the continuous wavelet transform (CWT), the wavelet family is derived from the base wavelet via expansion and translation. The CWT possesses the attributes of remaining invariant during translation and exhibiting simultaneous variation upon expansion, resulting in a notable connection among the CWT coefficients. The wavelet transform coefficients for two contiguous locations in the time-scale plane exhibit correlation. The proximity of the two spots correlates with the strength of the association. As the distance between the two spots expands, their correlation diminishes swiftly. This indicates that data redundancy exists in the signal's CWT, which complicates the analysis and interpretation of the wavelet transform results [42].

While the discrete wavelet transform (DWT) proficiently captures the singularity of one-dimensional signals, it does not perform similarly in two-dimensional scenarios. The two-dimensional orthogonal wavelet basis is constructed using the tensor product of two one-dimensional orthogonal wavelet bases, resulting in restricted direction selectivity.
The horizontal, vertical, and diagonal two-dimensional Discrete Wavelet Transform (DWT) fails to adequately represent the contour and edge information of the image; thus, DWT does not provide a sparse representation of these features. Its efficacy in image denoising, texture classification, and picture retrieval is inferior to that of multi-directional wavelet.

Wavelet coefficients can form a useful feature set; however, a basic limitation of the Discrete Wavelet Transform (DWT) is its lack of shift invariance. When the signal under analysis is moved, the coefficients of the wavelet transform exhibit complex variations. This issue poses a substantial challenge in the realm of pattern recognition. To address this issue, we can employ the shift-invariant characteristics of the Discrete Wavelet Transform (DWT), namely zero crossing (ZC) [49].

To develop the feature set with DWT, it was necessary to identify the parameters that influenced it. Consequently, we evaluate these parameters and compute the accuracy of the SEMG pattern recognition system, subsequently selecting the optimal settings. Two parameters must be established for DWT: the selection of the mother wavelet and the depth of decomposition. The optimal mother wavelet for SEMG pattern identification was established empirically. The selection of the mother wavelet should be predicated on optimal correlation with the EMG signal.

The DWT decomposition may be concluded before completing the entire process. If a signal has a length of N samples, then the maximum depth of decomposition is J =$\log_2$(N).The SEMG signal in this study comprises 500 samples, hence the maximum depth of decomposition will be 9.

2.2.3.2 Bases of Wavelet:

1) **Common Bases For Wavelets:**

The Haar wavelet is the earliest wavelet to be discovered and has the most basic form. It is a step function. Equation (3) illustrates its expression.

$$\Psi(t) = \begin{cases} 1, & 0 \le t < \frac{1}{2} \\ -1, & \frac{1}{2} \le t < 1 \\ 0, & Else \end{cases} \qquad (2,15)$$

In 1987, the Daubechies wavelet was developed. The primary benefit of the Daubechies wavelet is that it can be implemented using a finite impulse response conjugate mirror filter. Daubechies wavelets are typically abbreviated as dbN, where N denotes the wavelet's order. There is no closed-form expression for dbN. The Daubechies wavelet exhibits superior regularity. The vanishing moment of the wavelet increases as the order N increases, and its localization ability in the frequency domain is stronger. However, the quantity of computation also increases. Daubechies enhanced the wavelet system and developed the Symlets and Coiflets wavelets to achieve superior symmetry. Coiflet exhibits superior symmetry in comparison to dbN.

Symlet wavelet function is a wavelet function that is approximately symmetric and enhances the dbN function. In terms of continuity, they are consistent with the dbN wavelet.
Biorthogonal wavelets facilitate signal reconstruction and may precisely recreate the signal using a finite impulse response filter (FIR).

The Meyer wavelet differs from its predecessors.It is delineated in the frequency domain [33]. Despite possessing an analytical form, it lacks a compact support set.

Figure 3 illustrates many wavelet functions, including Haar wavelet, Daubechies wavelet, Biorthogonal wavelet, Meyer wavelet, Symlets wavelet, and Coiflets wavelet.

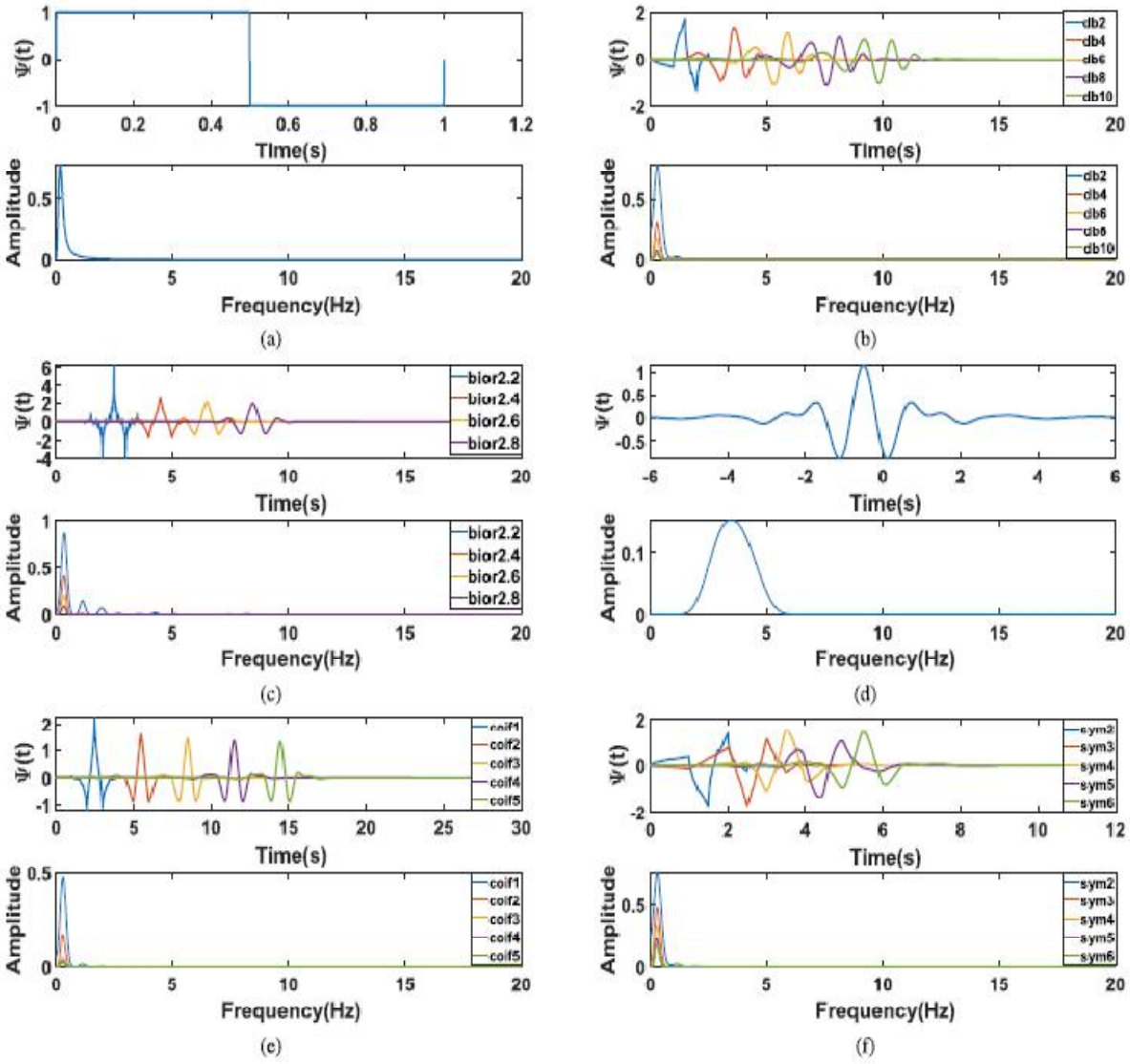

Figure 2.2: Various Wavelet functions and their frequency responses: (a) Haar wavelet; (b) Daubechies wavelet family; (c) Biorthogonal wavelet family; (d) Meyer wavelet; (e) Symlets wavelet family; (f) Coiflets wavelet family.

2.3. Empirical Mode Decomposition (EMD):

The empirical mode decomposition method is an innovative technique for the iterative decomposition of nonlinear, multicomponent time series signals. The decomposed time series functions, known as IMFs, display instantaneous frequency and amplitude characteristics as processed by the Hilbert transform. The EMD algorithm is derived from empirical concepts rather than analytical computations [50].

According to the EMD criteria, the IMFs must adhere to two constraints:

(a): The quantity of extrema (overshoots and undershoots) and the count of zero crossings in the signal must be identical or differ by at most one.

(b): The mean of the upper and lower envelopes, determined by the local extrema, should be uniformly zero. The local average is 0 at each place.

The EMD process is an iterative method that is computed in a systematic manner. The local extrema points are computed for the specified time series *signal x(t)* at the outset. The envelope signals corresponding to local minima (e_{min} (t)) and local maxima (e_{max} (t)) have been acquired. The subsequent step involves calculating the local average :

$$m(t) = [e_{min}(t) + e_{max}(t)]/2 \qquad (2,16)$$

The IMFs are computed recursively through the i parameter utilizing local averages.

$$c_i(t) = x(t) - m(t) \qquad (2,17)$$

The validity of the calculated IMF is assessed based on the previously mentioned criteria. If the IMF is not valid, the iterative process is repeated. If the IMF is valid, then it is established that IMF is equal to $z_1(t) = c_i(t)$.

$$x_1(t) = x(t) - z_1(t) \qquad (2,18)$$

This process is repeated for $i = 1$ to n, resulting in the completion of signal decomposition and the generation of IMFs.

2.4. Variational Mode Decomposition (VMD):

Variational Mode Decomposition is a systematic process that separates the given signal into distinct signal waveforms (modes). The center frequencies characterize these modes. The modes (c_k) are assessed for k values in accordance with a variational approach, ensuring that the sum of each mode (IMF) corresponds to the specified time series signal x(t). The Hilbert transform is performed to obtain the frequency spectrum for each mode [50].

$$\left(\sigma(t) + \frac{j}{\pi t}\right) c_k(\mathrm{t})$$

The computed center frequency is utilized to achieve spectrum shifting for each mode, with w_k representing the center frequency.

$$\left[\left(\sigma(t) + \frac{j}{\pi t}\right) c_k(\mathrm{t})\right] e^{-jw_k t}$$

The constrained variational evaluation for the specified signal x(t) is defined as follows:

$$\min_{c_k, w_k} \left\{ \sum_k \left\| \partial t \left[\left(\sigma(t) + \frac{j}{\pi t}\right) c_k(t) \right] e^{-jw_k t} \right\| \frac{2}{2} \right\}, \quad \sum_k c_k = x \qquad (2,19)$$

Where c_k=c_1,c_2,...c_k and w_k=w_1, w_2..... w_k are given.

Lagrangian multipliers are employed to resolve variational problems. In the solution provided, the unconstrained problem is resolved by employing a Lagrangian multiplier (dual ascent) ƛ and an aquadratic penalty term a [51,52].

$$\boldsymbol{L(c_k, w_k, ƛ) = \alpha \sum_k \left\| \partial t \left[\left(\sigma(t) + \frac{j}{\pi t}\right) c_k(t) \right] e^{-jw_k t} \right\| \frac{2}{2} + \|x(t) - \sum_k c_k(t)\| \langle ƛ(t), x - kCk(t)} \qquad (2,20)$$

The VMD process is implemented as an initial phase to calculate of C_k^1 , W_k^1 and λ^1. These values are subsequently updated(C_k^{n+1} , W_k^{n+1} and λ^{n+1}) for higher orders (n) in subsequent steps. The subsequent calculations are performed in the frequency domain, where the parameters are determined by.

$$C_K^{n+1} = \left[\hat{x} - \sum_{i \neq k} \hat{c}_i + \frac{\hat{\lambda}}{2}\right] \frac{1}{1+2\alpha\,(w - w_i)^2} \qquad (2,21)$$

The signal under analysis is decomposed into modes (c_k) using center frequencies (w_k) .

$$W_k^{n+1} = \frac{\int_0^\infty w\left|\widehat{c_k(w)}\right|^2 dw}{\int_0^\infty \left|\widehat{ck\,(W)}\right|^2 dw} \qquad (2,22)$$

The center frequencies are recalculated for each iteration, and each mode is updated in the frequency domain, as per the VMD algorithm.

2.5. Conclusion:

After data acquisition phase EMG signal features are needed to be extracted to specify the intended motion and force production. To achieve this task, this chapter presents various types of extraction features methods in time domain and frequency domain and in joint time-frequency domain.

The next chapter gives an overview on the widely employed classifiers in literature for classifying EMG signal.

CHAPTER 3

EMG Signal classification methods

3.1. Introduction:

Classifying extracted time or frequency domain characteristics is necessary to ascertain motion or applied force patterns. The primary focus of advancements in pattern recognition of myoelectric signals is that each force or motion category is characterized by the associated muscle activation, represented by a collection of extracted properties. The selection of an appropriate classifier for the pattern recognition process is a critical issue that aims to discover accurate patterns and ensure sufficient speed.

This chapter addresses the essential architecture and uses of commonly utilized classifiers, including ANN, FL, SVM, and LDA, for the control of myoelectric prosthetics.

3.2. EMG Signal Classification

The information generated from the EMG signals will thereafter be input into a classifier to identify and suitably match various patterns. Classifiers must be utilized to differentiate various categories of the extracted characteristics. The acquired categories will thereafter be utilized as control commands for the controller in the next phase. Various methodologies are utilized to categorize EMG data, including artificial neural networks (ANN), Bayesian classifiers (BC), fuzzy logic (FL), multilayer perceptrons (MLP), support vector machines (SVM), linear discriminant analysis (LDA), hidden Markov models (HMM), and K-nearest neighbors (KNN). Recently, numerous researchers have demonstrated interest in efficient methods for categorizing EMG signal patterns[53].

It was claimed in 1999 that classifier capabilities affect feature extraction and dimensionality reduction. The study classified hand gestures using LDA and MLP statistical classifiers. LDA performs best with 93.75% classification accuracy utilizing a PCA reduced feature set. They also found that the MLP may prescribe nonlinear class boundaries to cover the LDA's capabilities, giving it an edge. As indicated in [54], LDA classifiers outperform MLP classifiers for TFD-based features two years later [55]. Although the LDA does not need heuristic criteria for its architecture or training procedure, it consistently works well. This is likely because PCA dimensionality reduction linearizes the classifier's discrimination problem. Phinyomark et al. compared LDA, RFS, DT, KNN, SVM, and MLP-NN quadratic discriminant analysis (QDA) to classify ten upper limb motions in 2013. Based on TD characteristics, LDA achieved 98.87% classification accuracy. Khushaba and Al-Jumaily used MLP to classify human forearm motions using TFD characteristics with 99% accuracy [56].

Conversely, an ANN technique is appropriate for modeling nonlinear data because of its capacity to differentiate among many situations, such as hand motions (left, right, up, and down). The overall performance for a single trial was determined to be 89.2%, with an average success rate of 88.4% based on TD characteristics, as reported by Ahsan et al. [57]. However, the accuracy of ANN outputs is invariably constrained by the least square errors, as elaborated in [58]. Xie et al. asserted that the training duration of artificial neural networks is very lengthy, and the training data must be selected across a comprehensive spectrum where variables are anticipated to fluctuate. Furthermore, ascertaining the appropriate dimensions and architecture of an artificial neural network to address a specific issue is challenging.

Another method utilized in the classification of EMG signals is the FL system. FL offers a straightforward method to get a definitive conclusion using ambiguous input data that reflects a user's intent to make decisions based on biosignal features, which are not consistently reproducible. FL possesses a superior edge in control methodologies for biosignal processing [59]. The FL system fundamentally has three stages: input, processing, and output. During the input phase, referred to as the fuzzification module, the signal characteristics will be transformed into a state, known as the membership function (MF) and truth values, exemplified by upward and downward hand motions. During the processing step, sometimes referred to as the inference rule base stage, all information will be processed according to the rules specified in IF-THEN format. A suitable rule will be applied at this juncture, producing the outcome for each rule, which thereafter amalgamates the results of the rules. The output stage, possessing its own membership function, will subsequently transform the aggregated findings from the preceding stage into a definitive output value. This process is referred to as defuzzification. Despite the challenges in accurately determining the appropriate fuzzy rules and membership functions to characterize system behavior in fuzzy logic algorithms, a study by Ahmad and Chappel aimed at detecting wrist muscle contraction stages achieved a classification accuracy of 97% utilizing fuzzy logic as a classifier [51]. In 2015, Xie et al. [58] noted that while studies utilizing fuzzy logic (FL) systems employ IF-THEN rules that more accurately replicate human decision-making compared to other classifiers, there are criticisms regarding FL algorithms. They elucidate that fuzzy logic approaches necessitate more system memory and processing time, since the implementation of fuzzy logic constrains system knowledge more significantly inside the rule base than within the membership function base of fixed geometric-shaped membership functions.

Nonetheless, neuro-fuzzy systems computing facilitates the development of a more robust intelligent decision-making system by integrating the benefits of artificial neural networks with fuzzy modeling of imprecise and qualitative knowledge [42]. Hussein and Malcolm [60] utilized a neuro-fuzzy classifier to determine the desire of a paraplegic individual to either stand or sit based on single-site EMG signals acquired from the triceps and biceps brachii muscles for the purpose of electrical stimulation orthosis. This neuro-fuzzy hybridization was functionally grounded on a Sugeno-type fuzzy rule base combined with a radial basis function (RBF) neural network, subject to certain constraints to enable the system to learn from the training data. This classifier can detect 28 sitting and 29 standing EMG signals from a total of

60 EMG signals, utilizing seven bell-shaped membership functions and 30 rules. ANFIS is a neural network architecture derived from the Takagi–Sugeno fuzzy inference system. It has the capacity to amalgamate the advantages of both methodologies inside a unified framework by incorporating neural networks and fuzzy logic concepts. The Sugeno fuzzy model-based Adaptive Neuro-fuzzy system was employed to categorize seven unique movements over an extended test time of approximately three hours, with an average accuracy of 86% based on TD characteristics [33]. On real-time intelligent pattern recognition algorithms for surface EMG signals achieved an average accuracy of 97% in distinguishing six types of hand movements using the ANFIS method based on TFD features [42].

The SVM is a kernel-based method that has gained popularity for machine learning applications related to classification and regression. Support Vector Machine (SVM), a promising data categorization technology introduced by Vapnik [61], is derived from the training process utilizing the training data. Subsequently, classification is executed utilizing the trained model. The primary challenges faced in establishing the SVM model involve determining the appropriate kernel function and its parameter values. The bilinear model is developed to classify five hand gestures using SVM by combining two linear parameters that are depending on the user and the motion, facilitating numerous users to execute various movements. This technique achieved 73% accuracy, but a hybridization of particle swarm optimization (PSO) and SVM attained 96.75% [62] in the detection of neuromuscular diseases. The findings indicate that the kernel parameter configuration of Support Vector Machines in electromyography data classification utilizing time-frequency domain characteristics (Discrete Wavelet Transform) influences classification efficacy.

3.2.1. Artificial Neural Networks (ANN)

Artificial Neural Networks (ANN) are a form of artificial intelligence modeled after the biological architecture of the human brain, commonly known as "neural networks" . In the human brain, neural networks are important to the decision-making process. The receptors detect inputs from the external environment and convert them into electrical impulses for transmission to brain networks. Subsequently, neural networks process the information and render decisions. Ultimately, the decision is relayed to the effectors to transform the impulses into responses as outputs. Biological and artificial neural networks establish a linear or nonlinear relationship between inputs and outputs to produce a certain judgment [39].

The classification of surface EMG features utilizing artificial neural networks is a prominent topic in scientific research concerning the control of human arm prosthesis. Figure2.4 illustrates the fundamental architecture of the artificial neural network employed in the pattern recognition of EMG signals.

The structure, known as the multilayer perceptron (MLP), is one of the most straightforward and often utilized types of artificial neural networks. It is comprised of a set of one input layer, one output layer, and a number of hidden layers. A typical architecture of an artificial neural network that is utilized for the categorization of EMG signal features consists of input, hidden, and output layers. This structure is designed to allow the features to be associated with various force or position classes. An artificial neural network receives extracted EMG features as a set of inputs, and the inputs are then sorted into various force or motion classes as the set of outputs. A weighting factor, denoted by the letter w, is assigned to each connection that exists between neurons in neighboring layers, such as input/hidden layers and hidden/output layers. Furthermore, neurons in the hidden and output layers implement a transfer function in order to establish a mathematical relationship between the inputs and outputs of the network. There is the possibility of selecting the transfer function f(x) of input arrays x, which establishes a relation between input and output data arrays, in accordance with the peculiarities of the problem. As an illustration, the following is the formula for a logistic sigmoid transfer function:

$$f(x) = \frac{1}{1+e^{\beta x}} \qquad (3,1)$$

$$x = \sum_{n=1}^{k} w_n a_n$$

denotes the aggregate input of a neuron, where w_n, β and a_n represent the weight, coefficient, and input of the element, respectively. While other transfer functions exist, the logistic sigmoid and hyperbolic tangent sigmoid transfer functions are the most prevalent in the pattern detection of EMG signals. The quantity of layers and neurons is modifiable according on the findings obtained. The utilization of extensive training data and numerous neurons may result in over fitting, leading to a complicated network architecture that must perform additional functions, thereby causing delays. To address this issue, several dropout algorithms may be implemented, and the train-test data percentage is suggested to be modified.

Neural networks have been employed to derive the most accurate output values for aligning with real-world findings by adjusting the weights throughout the training phase. Weight adaptation is executed based on the expected outcomes, a process known as guided learning. In supervised learning of EMG signals, the intended outcomes may include location, hand/muscle force, joint torque, or motion trajectory. Artificial Neural Networks (ANN) have been utilized as classifiers to predict arm and joint trajectories, estimate hand and wrist motion trajectories in the control of a virtual hand, classify types of limb motion, recognize motion patterns based on signal time scale features, and predict the kinematics of the shoulder and elbow.

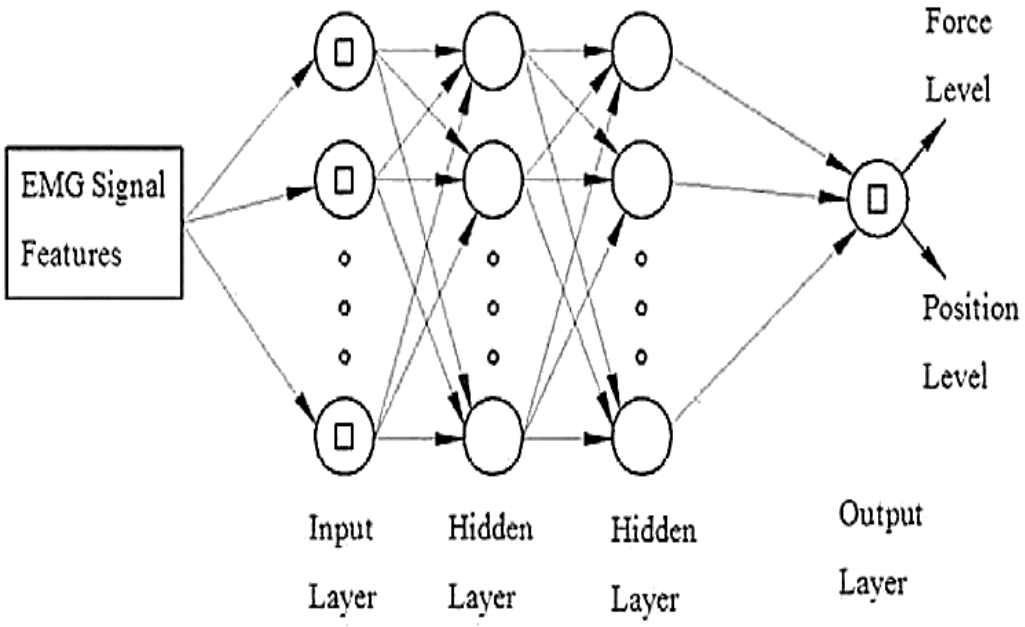

Figure3.1: Schematic representation of an artificial neural network

3.2.2 Fuzzy Logic (FL) System

Fuzzy logic systems are advantageous in signal processing and categorization, particularly for biological signals that are often non-repetitive and may even exhibit contradictions [63]. One of the most advantageous characteristics of fuzzy logic systems is their capacity to accommodate data disparities. Furthermore, trainable fuzzy algorithms can discern patterns in data that are not readily identifiable by alternative methods. Consequently, the expertise of medical professionals or clinicians could be assimilated and utilized effectively. This incomplete yet valuable knowledge can be integrated into the fuzzy logic system, owing to the system's reasoning approach, which resembles human cognition. This represents a significant advantage over the artificial neural network (ANN). Fuzzy logic systems more accurately represent human decision-making capabilities than artificial neural networks. The core component of a fuzzy system is the fuzzy inference engine. Fuzzy production rules are determined based on existing information or accurately classified examples .

In the fuzzy technique, all operations are deterministic. Information containing a degree of suspense is conveyed as reliably as feasible, without distorting it into a "crisp" structure, and is thereafter managed appropriately. Figure3.2 illustrates the schematic representation of a fuzzy logic system, encompassing the fuzzifier and defuzzifier stages.

Fuzzy Logic Systems architecture has three main Figure 3.2 These are:

1. Fuzzification Module (converts system inputs into fuzzy sets).
2. Fuzzy Inference Engine (emulates human decision-making by performing fuzzy inference on the inputs).
3. Defuzzification Module (converts fuzzy sets into output parameters).

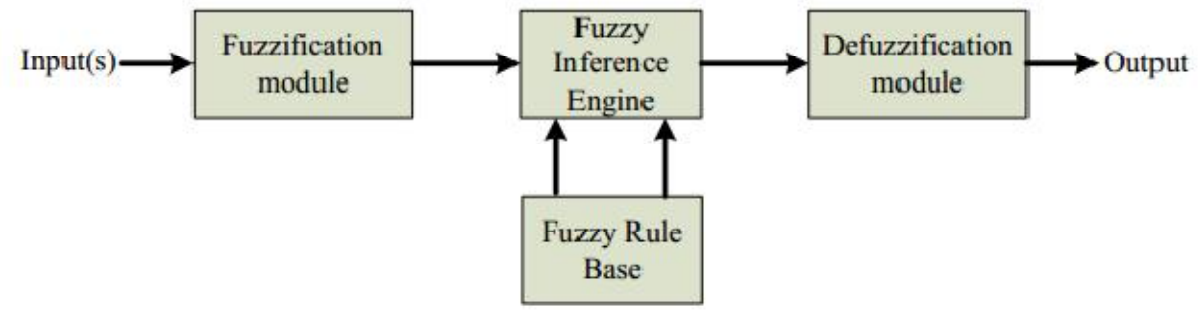

Figure 3.2: General block diagram for FL systems.

The inference engine correlates the fuzzy input sets of each rule with the corresponding fuzzy output set of that rule. Regulations significantly impact the efficacy of a federated learning system. The rules function just when the inputs are implemented.

A dataset is utilized to train a fuzzy logic system for rule prediction. A specific quantity of input-output training pairings is chosen. The subsequent stage involves transforming the training dataset into a collection of fuzzy rules (IF-THEN, IF-THEN-ELSE, etc.).

The fuzzy rules establish a quantitative mapping from the inputs to the outputs. This type of fuzzy logic system is prevalent and extensively utilized across various engineering applications, including fuzzy logic controllers and signal processing units. It is referred to as a fuzzy system, fuzzy controller, fuzzy model, or fuzzy expert system.

Recent advancements indicate that FL systems have been employed in the decision-making processes within biomechanical science. The FLS system has been utilized to regulate the elbow and shoulder joint angles of exoskeletons for the purpose of designing a controller for multifunction prosthetics[64].

3.2.3 Support Vector Machine (SVM)

Support vector machines (SVM) represent a contemporary and advanced approach in machine learning. The EMG-based classification process for prosthetic control necessitates high accuracy and rapid output generation, leading to the widespread adoption of SVM as a classifier. The primary objective of the classification process is to assign inputs to predefined groups or categories; however, Support Vector Machines (SVM) fundamentally separate classes by utilizing an optimal hyperplane. A combination of multiple SVMs is employed to differentiate data across numerous classes. The SVM classification process is succinctly outlined as follows [65].

Let x_i and y_i are inputs and outputs, respectively, for $x_i \in R^i \; and \; y_i \in \{-1,1\}^l$

The hyper- plane, which divides them into two previously determined groups, is defined as:

$$w^T \phi(x) + b = 0 \qquad (3,2)$$

w and b represent the weight and bias parameters of the hyperplane. Furthermore,ϕ serves as a mapping function that transforms the x_i vector into a higher-dimensional space.

In a classification scenario, multiple hyperplanes can effectively partition data into two distinct classes. However, there exists a unique hyperplane that maximizes the margin between the classes, defined as follows:

$$min\left[\frac{1}{2}\|w\|^2 + C\sum_{i=1}^{m}\xi_i\right] \qquad (3,3)$$

Subject to $y_i(w\phi(x_i) + b) \geq 1 - \xi_i$ and $\xi_i \geq 0$ where ξ_i is the slack variables that related to error between training data.

In order to obtain optimal hyperplane with limited error equation, equation (3.2) is solved, while $a_i$and $K(x_i, x_j)$are Lagrange multipliers and Kernel function, respectively, the equation is reduced as follows:

$$max\left[\left[\sum_{i=1}^{\infty} a_i - \frac{1}{2}\sum_{i,j=1}^{m} a_i a_j y_i y_j k(x_i, x_j)\right]\right. \qquad (3,4)$$

The equation of optimal hyperplane is expressed as:

$$w = \sum_{i=1}^{m} y_i\, a_i \phi(x_i, x_j) \qquad (3,5)$$

This satisfies:

$$\sum_{i=1}^{m} a_i\, y_i = 0,\ and\ 0 \leq a_i \leq C \qquad (3,6)$$

The inputs x_i which satisfy $a_i \neq 0$are called support vectors. The maximization process to build decision function of the classifier is related to choose suitable kernel function which is generally selected based on inputs type and structure [66].

The most common used kernel functions are linear, polynomial, sigmoid and radial basis functions. The major components of SVM are shown in Figure 3.2.

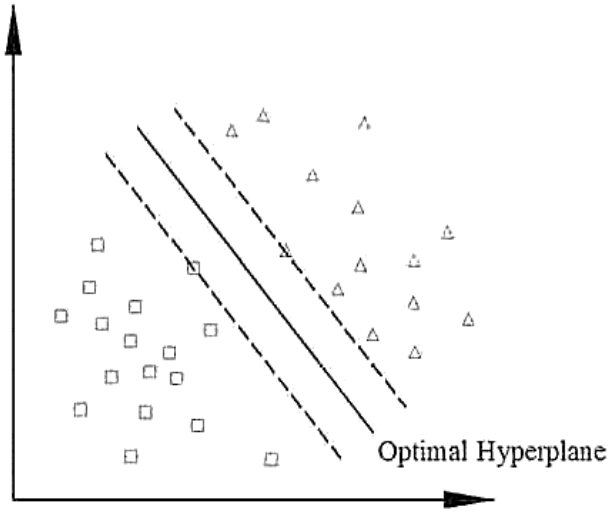

Figure 3.3: SVM's fundamental form: Solid line represents optimal hyperplane, dividing optimal margin between classes. Square and triangle on dashed lines support vectors.

The use of SVM method as a supervised classification of multi-channel surface electromyographic signals with the aim of controlling myoelectric prostheses confirm that the SVM classification rule can be effectively implemented with fast algorithms (after training) for real-time applications [50].

3.2.4 Linear Discriminant Analysis (LDA)

Linear discriminant analysis (LDA) has emerged as a prominent classifier with the objective of organizing extremely intricate EMG data arrays. The method is predicated on the identification of the parameters that are most effective in distinguishing the predetermined categories [39].

It is assumed that the vector of features is given as $X = [x_1, x_1, \ldots, x_m]$.

The mean values of X for the i^{th} class are expressed as $\mu_i = [\mu_{i1}, \mu_{i2}, \ldots, \mu_{im}]$.

The primary technique of the LDA approach is to optimize the following function, referred to as the linear discrimination or gate function.

$$f_i(x) = x^T S^{-1} \mu_i - \frac{1}{2} \mu_i^T S^{-1} \mu_i + log(\pi_i) \qquad (3,7)$$

S represents the pooled covariance matrix of the input data, while π_i denotes the prior probability of the inputs originating from class i. By utilizing the combinations of the equation, misclassification can be reduced by achieving a higher likelihood index for each specified class.

The LDA method has been utilized to identify EMG signals for distinguishing the EMG linear envelope patterns of healthy individuals and patients with anterior cruciate ligament injuries, as well as to classify features to improve the controllability of powered prosthetics.

An detailed review of the performance of the specified classifiers in the pattern recognition process, along with their faults and merits, is essential.

The use of artificial neural networks to forecast externally applied stresses on human hands by analyzing EMG data characteristics demonstrated that the classifier predicted the target force values with a root mean square difference (RMSD) ranging from 0.34 to 0.05 for isometric contractions and from 0.24 to 0.09 for an isometric contractions. This study explicitly indicated that the ANN approach could establish a successful non-linear relationship between force and EMG signal characteristics. Nevertheless, the authors emphasized that a standardized ANN design for the efficient training of EMG signals cannot be proposed. Despite the efficacy of ANN as a classifier, the lack of a defined and uniform training methodology constitutes a significant drawback [67].

A comparison between artificial neural networks and fuzzy systems in the pattern identification process shown that Fuzzy and ANN classifiers achieved error rates of 8% and 11.3% in pattern identification, respectively [68].

The advantages of fuzzy systems include:
Marginally superior recognition rate compared to that achieved by ANN, insensitivity to overfitting, and consistent outputs indicating enhanced reliability. The primary disadvantage of the method was identified as necessitating increased human intervention during the initialization phase to achieve minimal inter-class crossover. Consequently, it was indicated that the technique is not as automated as ANN [69].

LDA is emerging as a significant instrument for pattern detection in electromyography (EMG) research. Like the work [70] performed a study that encompasses an EMG feature discrimination procedure and in [71] shown that LDA outperforms other classifiers, including quadratic discriminant analysis (QDA), random forests (RFs), and k-nearest neighbor (KNN), in the categorization of fluctuating EMG data.

3. 3. Conclusion:

The purpose of this chapter is to provide a comprehensive overview of pattern identification and classification methods of electromyographic (EMG) data. These approaches are particularly significant in a wide variety of applications, including rehabilitation devices, prostheses, orthoses, and the detection of neuromuscular disorders.

In the following chapter, we will show our proposed approach for classifying EMG signals, which is based on LDA and ANFIS in addition to the findings that were obtained.

CHAPTER 4

EMG Signal Classification results

4.1. Introduction

This chapter presents the dataset and our proposed method to classify the EMG signals additionally the results achieved.

The outline of this chapter is structured as follows: first, we present the materials and methods used to acquire the dataset using an EMG muscle sensor and the MPU6050 board; then, a method is proposed to analyze EMG signals based on wavelets. After that, extracted features are displayed as feature vectors to be exploited by an LDA and ANFIS classifiers to estimate the forearm flexion angles and predict the human forearm movement. Finally, the study findings are discussed.

4.2. EMG signal classification system

The EMG data were collected using a Myoware muscle sensor (AT-04-001) connected to MPU6050 sensor, Processing of collected data, feature extraction, and classification were performed using MATLAB. First, the collected EMG data were filtered to reduce noise from data. From windowed datasets, different signal features were extracted. The features from different sets of EMG signal data were used as training and testing features for classification. Preferred classifier was Linear Discriminant Analysis (LDA) classifier because of its simplistic, efficient and fast classification, an adaptative neuro-fuzzy inference system was also utilised in order to estimate the angle flexion forearm. The study paradigm of this research work is presented in Figure 4.1

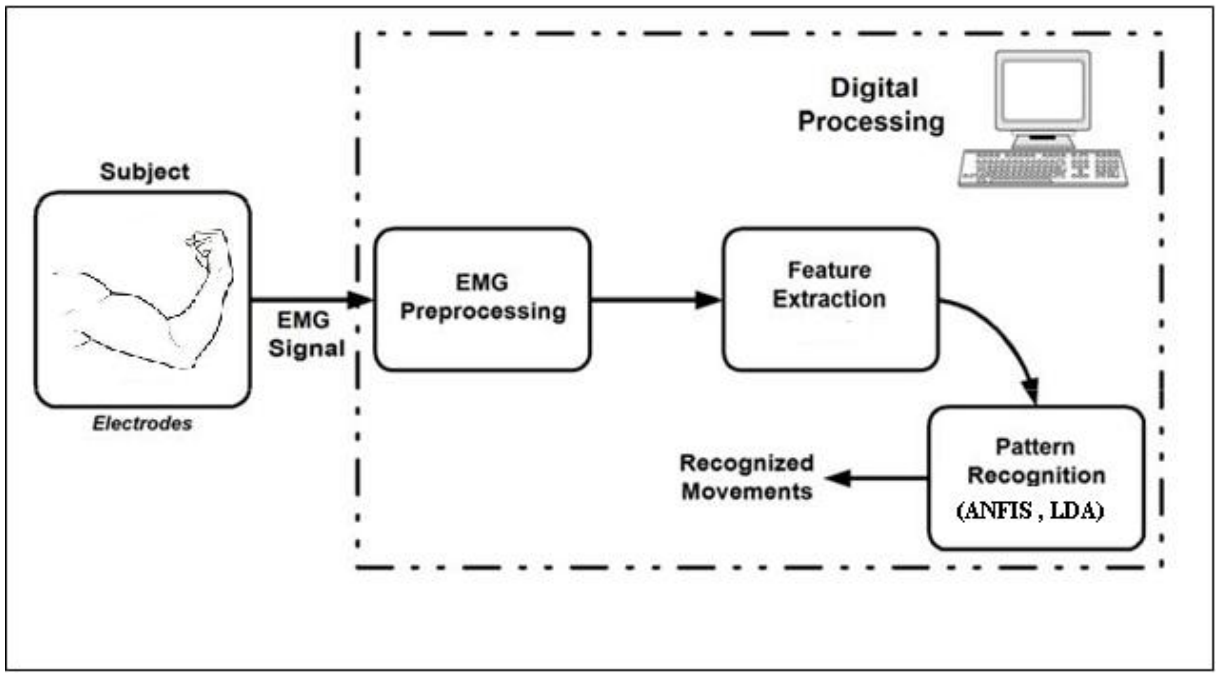

Figure 4.1: Flowchart of the proposed system

4.2.1. Dataset collection

Electromyography (EMG) signals were meticulously collected using a Myoware muscle sensor (AT-04-001) operating at 1000Hz, which was connected directly to a computer via the USB port using a digital oscilloscope (Hantek 6022BE). The data gathering involved ten volunteers in healthy conditions, comprising two males and eight females, aged between 25 to 40 years. In this study, we acknowledge the findings of Graupe et al. [72], which highlighted the considerable variations in EMG records for the same movement taken from different patients even under identical conditions. To maintain consistency, we focused our analysis on EMG data obtained specifically from the right bicep Figure 4.2

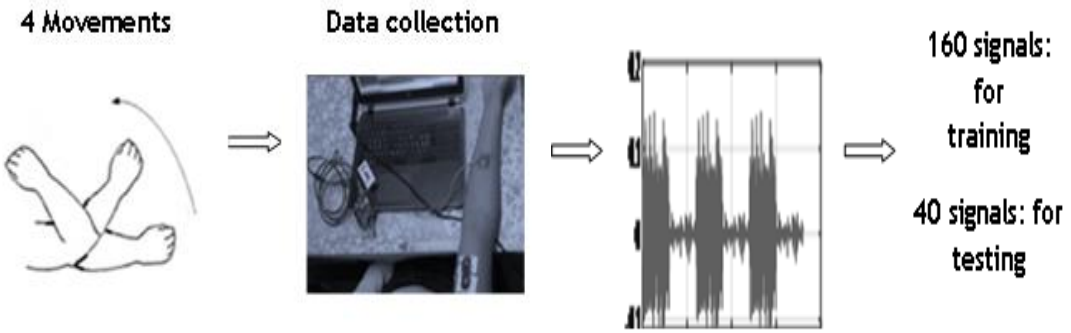

Figure 4.2: EMG data acquisition diagram

4.2.1.1 Myoware Muscle Sensor (AT-04-001)

The myoWare Muscle Sensor (AT-04-001) in Figure 4.3 is the new electromyography (EMG) sensor developed by Advancer Technologies. It is used to measure electrical activity that has been filtered and rectified in the muscle. This new version has the ability to output an amplified raw EMG signal.

To output the raw EMG signal, simply connect the raw EMG signal pin to your measuring device instead of the SIG pin. This output is centered about an offset voltage of +Vs/2; this will assure that you completely see both positive and negative portions of the waveform.

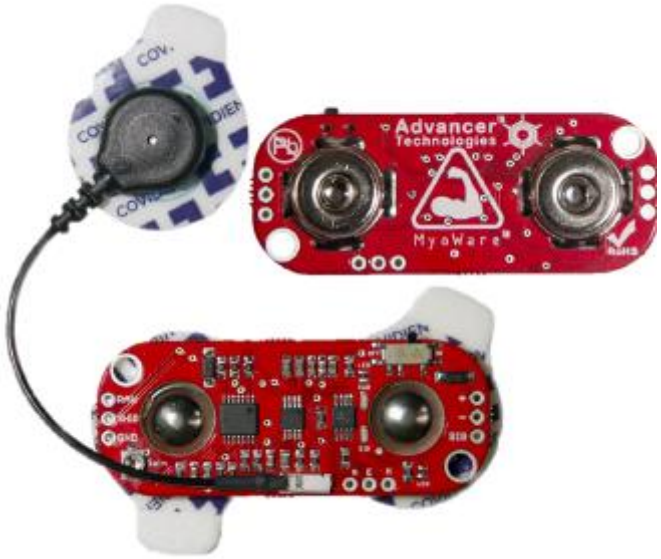

Figure 4.3: Myoware Muscle Sensor (AT-04-001)

The Myoware muscle sensor with the characteristics mentioned in Table 4.1 consists of three detecting surfaces strategically positioned at the muscle belly Figure 4.4. Two of these electrodes were placed within 1-2 cm of each other, deliberately away from the tendon and motor unit [73]. This positioning enabled the detection of the most active muscular groups during various trials. The third electrode served as the reference point and was placed on the adjacent bone.

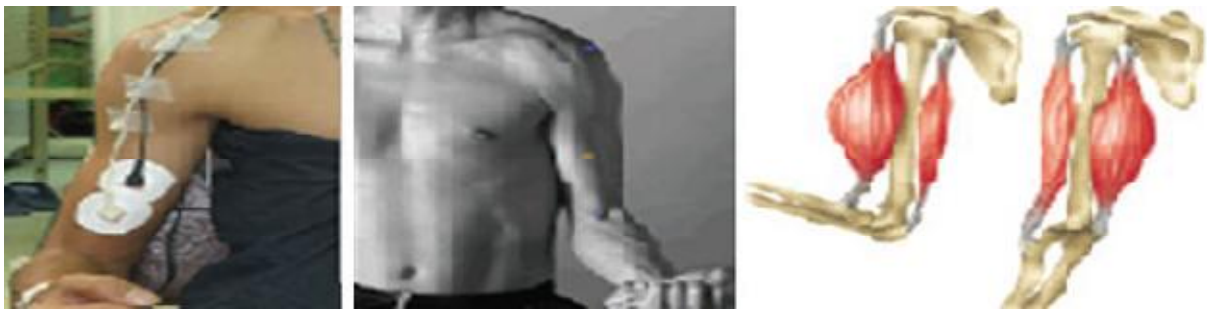

Figure 4.4: Biceps anatomy and electrode placement.

Table 4.1: MyoWare muscle sensor characteristics

Input type	±1.5 mv
Type of electrodes	Disposable Ag/AgCl
Number of channels	1
Output type	0–5V envelope Differential (±2.5 V)
Power supply	External
Weight	9 g
Output accessibility	Easily accessible
Price	$37.95

4.2.1.2 Electrodes

An electrode plays a crucial role in detecting ion migration on the tissue surface and converting it into an electric current that flows through a wire to a measuring device.

In selecting electrodes for various applications, several specific criteria are taken into consideration, such as the nature and cost of the electrodes, the origin of the bio-potential, and the signal-to-noise ratio (SNR).

Extensive research in this field has consistently shown that silver/silver chloride (Ag/AgCl) electrodes stand out as the optimal choice due to their remarkable attributes. These electrodes exhibit a low half-cell potential of approximately 220mV, ensuring reliable and accurate measurements. Additionally, Ag/AgCl electrodes offer the advantage of minimal noise and exceptional stability, further enhancing their effectiveness.

The (Ag/AgCl) electrode is designed in a bipolar configuration, making it surface-friendly and non-invasive. However, the passive use of an electrolyte conductive paste is necessary to

ensure optimal performance [74]. This combination of features makes (Ag/AgCl) electrodes a preferred and reliable choice in a wide range of applications.

4.2.1.3 MPU6050 IMU board

The MPU6050 board serves as a crucial component in detecting muscle motion and transmitting data to the microcontroller for further processing, specifically to calculate the angle of muscle flexion.

To achieve this, we securely fixed the MPU6050 board horizontally onto the forearm muscle. As the user moves their forearm around its axis, the gyroscope and accelerometer sensors integrated into the IMU board calculate the rotation and acceleration rate of the movement, providing raw values [75].

To ensure precise control of the system, we focused on forearm movement along the y-axis, while disregarding movement around the x and z-axes. The data related to the y-axis movement is then transmitted to the microcontroller, where we employ complex geometry to accurately calculate the proper angle [76].

Before proceeding with analysis, it is necessary to convert the raw data obtained from the MPU6050 sensor into angular values. Additionally, we determined the Pitch angle by using the accelerometer values along the y and z-axes. These measures facilitate more accurate assessment and interpretation of the muscle flexion angle during the study.

$$\theta_a = atan2(a_y, a_z) \qquad (4,1)$$

Data from the gyroscope are found in a similar manner, except that the output for the gyroscope represents angular rates in deg/s with a sensitivity factor of 14.375.

$$\dot{\theta} = \dot{\theta}_{prev} + \dot{\theta}_{new}.\Delta t \qquad (4,2)$$

Where

$\dot{\theta}$: is the pitch rate of the gyroscope.

Δt: is the unit of time.

Figure 4.5: MPU6050 IMU board

4.2.1.4 Arduino Uno

Arduino is an open-source microcontroller that is simple to program, based on the ATmega328P with 14 digital input/output pins, six of which can be exploited as PWM outputs and six analog inputs, as well as a USB connection. The microcontroller can be simply activated by connecting it to a computer via a USB cable or via an AC-to-DC adapter or battery [77].

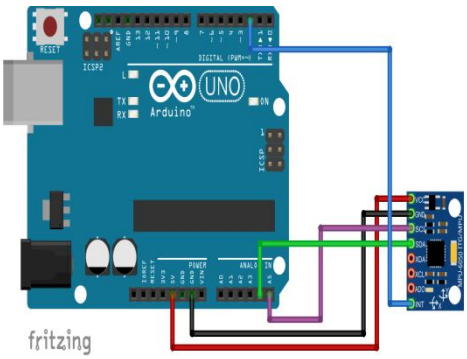

Figure 4.6: MPU6050 IMU board communicated to Arduino

To visualize and collect the signals effectively, we connected the EMG sensor to the Hantek 6022BE Oscilloscope. This setup allowed us to efficiently visualize and record the EMG signals for further analysis.

Figure 4.7: Proposed acquisition system

As shown in Figure 4.7, the connected sensor MPU6050 board to the Arduino was fixed horizontally at the right forearm to capture the exact angle of muscle flexion.

To acquire the necessary data, we selected four distinct gesture classes Figure 4.8:

relaxed muscle without elbow flexion at 0°
contracted muscle without elbow flexion at 30°
contracted muscle with elbow flexion at 90°
contracted muscle with elbow flexion at 120°

In order to minimize the influence of noise, the target muscle area was cleaned with a 70% isopropyl alcohol-containing alcohol swab. During the experiment, the volunteers were comfortably seated in chairs.

Figure 4.8: Selected muscle motions for classification

Each movement was performed five times by each volunteer.

To ensure comprehensive data collection and prevent any loss of valuable information, we introduced a four-second repose period both at the beginning and end of each contraction period. This approach effectively minimized data loss while facilitating the collection process.

Subsequently, to enhance the quality of the collected EMG signals and minimize noise interference from the skin at the electrode placement, we applied a Butterworth filter. The filter had a cutoff frequency of 50Hz and 450Hz, effectively eliminating unwanted noise while preserving the integrity of the signal for thorough analysis.

A 600-ms time window was used for the EMG signals collection during the data acquisition step.

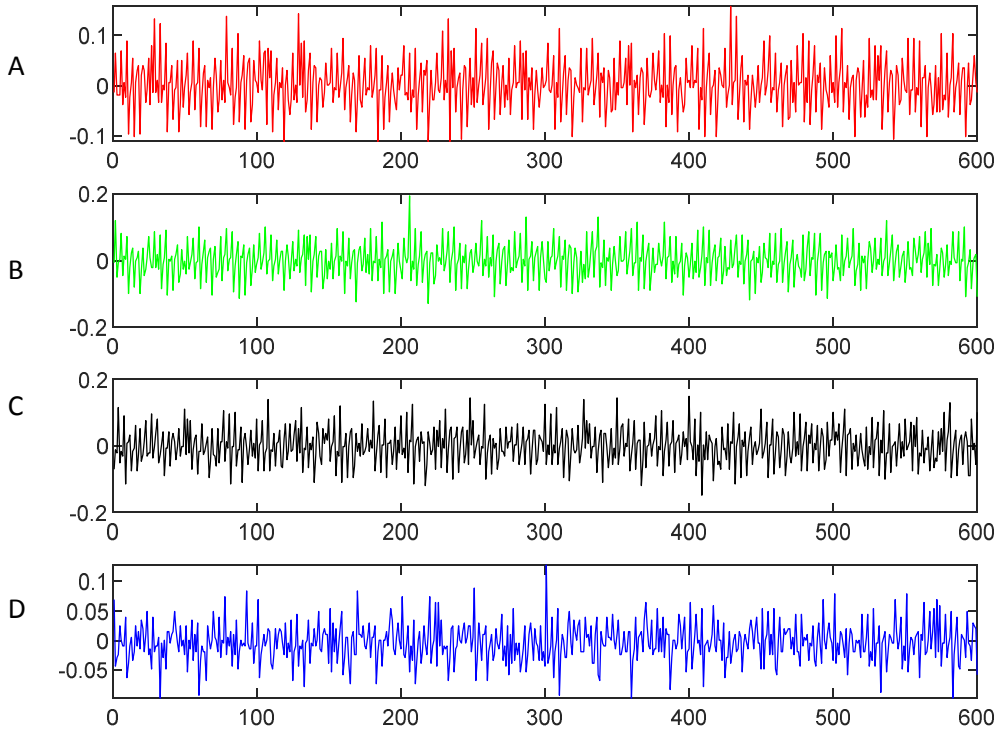

Figure 4.9: EMG signal records (A: Relaxed forearm at 0°, B: Flexed forearm at 30° C: Flexed forearm at 90°, D: Flexed forearm at 120°)

4.2.2 Feature Extraction

4.2.2.1 Discrete Wavelet Transform Characteristics

In our analysis, we conducted an off-line examination of the EMG signal using MATLAB 2021a and employed the wavelet transform technique.

The wavelet transform is a powerful method that involves dividing the signal into distinct kernel functions known as wavelets. These wavelets are derived from a fundamental function called the mother wavelet. By translating and scaling the mother wavelet appropriately, we can achieve a meaningful analysis of the signal. Wide wavelets are employed for low frequencies, while weak wavelets are utilized for high frequencies, allowing us to capture both global and localized features within the signal.

For the successful analysis of EMG signals, we carefully selected the Daubechies' family (db) function as the mother wavelet. This decision was crucial as the choice of the mother wavelet significantly impacts the analysis outcome, making the Daubechies' family an ideal

candidate for EMG signal analysis [78].

The wavelet transform can be defined as follows (eq.3)

$$(\alpha, \beta) = \int_{-\infty}^{+\infty} x(t) \frac{1}{\sqrt{\alpha}} \varphi(\frac{t-\beta}{\alpha}) dt \qquad (4,3)$$

Where

φ : is the transforming function (mother wavelet).

a : is the translation parameter.

β : is the scale parameter.

In the context of the discrete wavelet transform (DWT), the signal undergoes a process where it is filtered through both low and high pass filters. This filtering leads to the derivation of approximation coefficients, achieved through down-sampling to half the output of the low pass filter (LPF), and detail coefficients, obtained by down-sampling to half the output of the high pass filter (HPF). The LPF and HPF outputs are calculated using Eqs. (4) and (5), respectively.

$$y_{LPF}[n] = \sum_{k=-\infty}^{+\infty} x\,[k]\; l\,[2n - k] \qquad (4,4)$$

$$y_{HPF}[n] = \sum_{k=-\infty}^{+\infty} x[k]\; h[2n - k] \qquad (4,5)$$

y_{LPF} is the LPF output.

y_{HPF} is the HPF output.

x is the signal.

In the DWT process, decomposition levels are achieved by passing the signal through a pair of filters (LPF and HPF). To estimate the next decomposition level, the approximation coefficients from the previous level are passed through the LPF and HPF filters and then down-sampled to generate the new level's coefficients.

In this study, a second-level decomposition was employed to enable the extraction of EMG features using DWT. The discrete wavelet transform provided valuable information, which was further synthesized into one of the following values: root mean square, standard deviation, or mean absolute value. These feature choices were based on their demonstrated effectiveness in achieving desirable results.

A sample of an EMG signal recorded using a MyoWare muscle sensor and its wavelet transform coefficients at detail 2 are shown in Figure 4.10

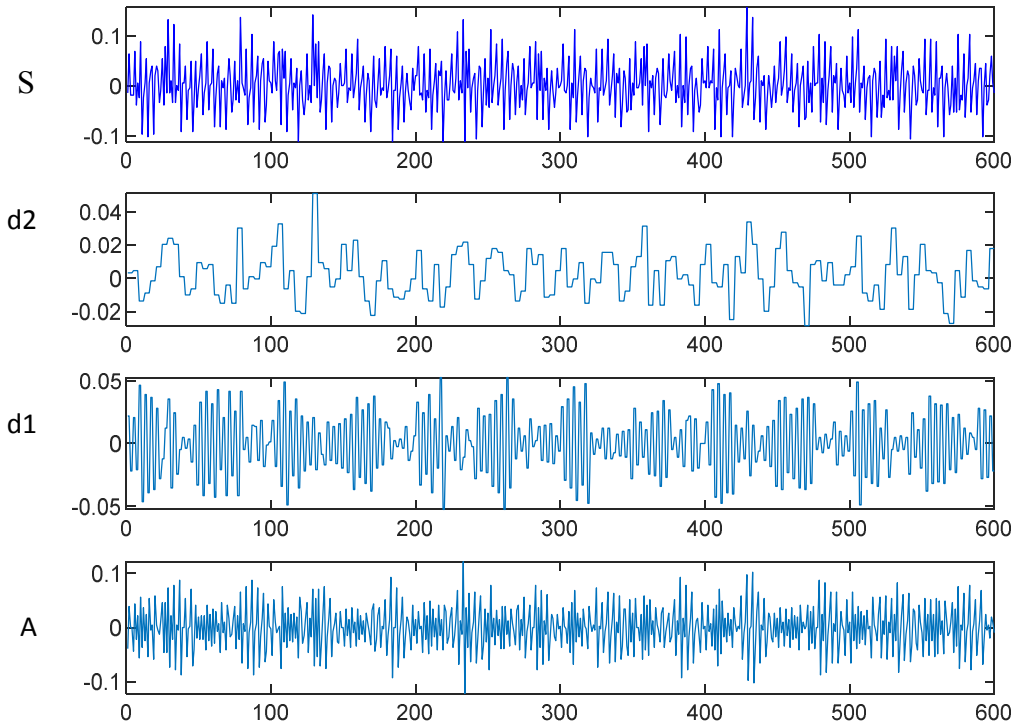

Figure 4.10: A sample of the EMG signal and its DWT signal.

The wavelet transform coefficients (detail 2) are obtained using Daubechies order 2 as the mother wavelet from the EMG signal of a contracted muscle with elbow flexion at 60°.

Figure 4.10 shows that the second detail coefficients closely resemble the original EMG signal. This implies that full information is kept in those coefficients. Hence, for the EMG signal analysis, detail 1 (d1) or detail 2 (d2) coefficients were sufficient to give the maximum number of features needed to represent the EMG signal for classification purposes. Therefore,

root mean square, mean absolute value, and standard deviation values are computed only from d2 coefficients besides the feature values (RMS, MAV, and STD) calculated directly from the EMG signal to form the feature vector and train it with the LDA classifier. Using the powerful software MATLAB, we find a good result with Daubechies order 2 as the mother wavelet at decomposition level 2.

4.2.3 EMG signal classification

4.2.3.1 LDA Classifier

We used linear discriminant analysis as a classifier because it is a prominent tool for EMG pattern recognition due to its high classification accuracy compared to other classifiers [79, 80].

The LDA classifier is linear and does not require iterative training which reduces computational time. It is based on the Bayes classification rule, which assigns a vector x to the class c_k if the following equation is satisfied:

$$p(c_k|x) > p(c_j|x) \quad for\ all\ k \neq j \qquad (4,6)$$

The probabilities presented in equation 9 are not computed directly. Instead, they are derived from the estimation of a priori probabilities and the class distribution, utilizing the Bayes equation.

$$p(c_k|x) = \frac{p(c_k)p(x|c_k)}{p(x)} \qquad (4,7)$$

Where

$p(x|c_k)$ is the probability density function.

$p(c_k)$ is the prior probability for class k.

$p(x)$ is the probability density function of the input space

After that, the decision rule illustrated in (eq. 6) is simplified to (eq. 8):

$$p(x|c_k) > p(x|c_j) \quad for\ all \quad k \neq j \qquad (4,8)$$

In the implementation of the LDA classifier, it is assumed that the probability density functions for each class follow a multivariate Gaussian distribution:

$$p(x|c_k) = \frac{1}{\sqrt{(2\pi)^f\ det(C))}} exp\ (-\frac{1}{2}(x-\mu_k)^T C^{-1}(x-\mu_k) \qquad (4,9)$$

Where

x: is the feature vector

f : is the vector dimension

c: is the common covariance matrix

μ_k : is the mean value of class *k*

The key training computation for the LDA classifier was to find the mean vector, the common covariance matrix, and the inverse matrix. Then, the classifier compares the testing matrix to the training matrix to select the suitable classe.

Sample values of computed features and the LDA classifier accuracy are illustrated in Table 2.4

Table 4.2: Average classification accuracy using LDA with RMS, MAV and STD features

Length of signal	TD features (MAV,STD,RMS)	LDA(%) Accuracy	TFD features (MAV,STD,RMS)	LDA(%) Accuracy	TD,TFD features	LDA
500samples	M1: 0.0393, 0.0508 0.7730	95	M1: 0.0479, 0.0598 0.5374	87.50	M1: 0.0393,0.0508,0.7730 0.0598	97.50
	M2: 0.0405, 0.0530 0.8410		M2: 0.0501, 0.0618 0.5732		M2: 0.0405, 0.0530, 0.8410 0.0618	
	M3: 0.0423, 0.0538,0.8663		M3: 0.0515, 0.0624 0.5841		M3: 0.0423, 0.0538, 0.8663 0.0624	
	M4: 0.0245,0.0317, 0.3003		M4: 0.0277, 0.0360 0.1953		M4: 0.0245, 0.0317,0.3003 0.0360	

Features include the mean absolute value, standard deviation, and root mean square values,

which are calculated for every sample of the four EMG signals used (M1, M2, M3, and M4). About 80% of the gathered signals are selected and used to train the LDA classifier. Conversely, 20% of them are used to test the same trained LDA for the forearm angle flexion estimate.

The combined (RMS, MAV, and STD) features extracted directly from the EMG signal are exploited by the LDA classifier with an accuracy of 95%. This outcome is higher than the use of the feature combination set RMS, MAV, and STD calculated from the discrete wavelet decomposition coefficients (detail 2) with an average classification accuracy of 87.50%.

The (MAV, RMS, and STD) values extracted from the signal EMG, with the STD value computed from the time-frequency domain features of the 2nd detail coefficients of the Daubechies order 2 with an average accuracy of 97.50%. Nevertheless, the mean absolute or integrated EMG values from the 2nd detail coefficient wavelet transform and the extracted domain features from the signal EMG does not affect the average classification accuracy and is still 95%.

Table 4.3 compares the classification of EMG to similar studies.

Table 3.4: Related studies in comparison to the proposed method

Reference	Channels num	Classifier	The window time (ms)	Gestures	Features	Accuracy
Proposed method	**1**	**LDA**	*500*	**4**	**MAV, RMS and ,STD Extracted from EMG signal and its DWT.**	**0.9750**
The work of Fajardo et al [6].(2021)	**1**	**LDA**	*750*	**4**	**Handcrafted features** **COMBINED FEATURES**	**0.8476** **0.9600**
The work of Zhang et al[41].(2017)	**8**	**SVM**	**256**	**14**	**DASDV,WTM, VORDER,LOG, WL, MDF, MAV, RMS, SM3, VAR, SSC, ZC, MDA, WTSVD, WPTM, WPTSVD, SSI, MYOP,**	**0.7020**
The work of Chen et al [42].(2017)	**6**	**SVM**	**5000**	**17**	**RMS, SSC, Willison Amplitude, Var, WL SSI, MAV, IEMG, ZC.**	**0.9508**
The work of Sheng et al[14].(2019)	**8**	**LDA**	**200**	**11** **9** **7**	**ZC, SSC, WL, MAV.**	**0.6383** **0.7284** **0.8603**

These studies used a variety of features and classifiers. In each study, it is necessary to emphasize the number of channels used while gathering data, and the examined window's duration. Utilizing a single EMG channel and a 500 ms sliding window, the proposed method provides good accuracy. Whereas work done by [81] improved performance for four gestures and one EMG channel using an LDA classifier, for a window of 750ms, which is too long for a real application of HCI or prosthesis control. Furthermore, the work done by [82] yields high performance for 17 gestures with an SVM classifier. However, this method employs six EMG channels and a long time window of 5s.

Works by Zhang et al. [83] and Sheng et al. [84] attain low accuracy even with LDA and SVM classifiers for an approximately similar time window using eight EMG channels.

4.2.3.2 Neuro-Fuzzy Classifier

The suggested ANFIS model was implemented in MATLAB using (MAV, STD, RMS) as inputs and one output.

The ANFIS model uses 5 Gaussian-type input membership functions for the three feature ranking parameters Figure 4.11

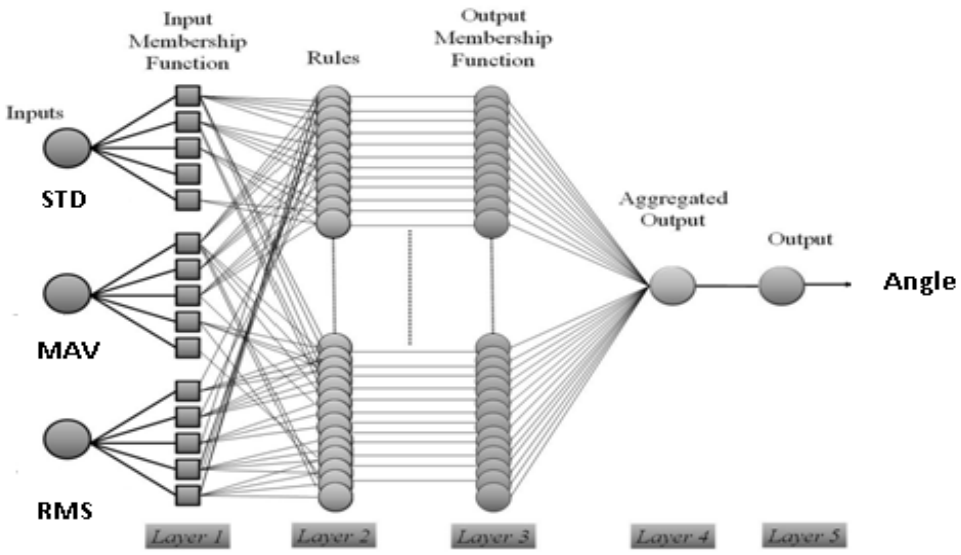

Figure 4.11: The suggested ANFIS model for muscle gesture classification

The Matlab function generated the first FIS. This enables fuzzy inference systems to learn from the data being modeled. 80% of the gathered data was used to train the ANFIS model. In contrast, 20% of them are employed to evaluate the same trained ANFIS for forearm angle flexion estimation.

Sample values of computed features and the ANFIS classifier results are illustrated in Table 4.4

Table 4.4: Classification outcomes using ANFIS

ANFIS inputs: MAV, STD, RMS	ANFIS output	Range	Estimated angle	The real angle Flexion	Classe
0.2226, 0.0168, 0.0176	13.50°	angle≤15°	0°	0°	1
0.2391, 0.0178, 0.3396	2.11°	angle≤15°	0°	0°	1
0.3051, 0.4002, 0.0094	31.90°	60°≥angle> 15°	30°	30°	2
0.2591, 0.0186, 0.3864	-15.62°	angle≤15°	0°	30°	1
0.2924, 0.0261,0.0200	93.85°	105°≥angle> 60°	90°	90°	3
0.3538, 0.0238, 0.3721	89.99°	105°≥angle> 60°	90°	90°	3
0.0806, 0.0165, 0.1223	89.58°	105°≥angle> 60°	90°	120°	3
0.0864, 0.1230, 0.0165	105.37°	angle> 105°	120°	120°	4

The ANFIS output classified the four forearm gestures with different angle values as follows:

- If the ANFIS output (Angle) ≤15°: The forearm is relaxed at 0° (classe 1)
- If the ANFIS output 60°≥angle> 15°: The forearm is flexed at 30° (classe 2)
- If the ANFIS output 105°≥angle> 60°: The forearm is flexed at 90° (classe 3)
- If the ANFIS output angle> 105°: The forearm is flexed at 120° (classe 4)

4.3.Conclusion

This chapter is organized as follows: The first part provides an overview of the various hardware and software used for EMG signal classification, which involves three stages: acquiring the EMG signals, extracting features from the signals, and performing classification. The second part focuses on presenting the outcomes obtained by utilizing ANFIS and LDA classifiers. The results were highly satisfactory. However, specific improvements are still necessary to achieve the desired level of quality.

CHAPTER 5

2 DOF Arm Manipulator Control Simulation and results

5.1. Introduction

This chapter presents the results and simulation of a planar two-degree of freedom (2-DOF) arm manipulator control. MATLAB is used to model the kinematics and visualize the manipulator configuration for given joint variables. The objective is to validate the theoretical kinematic equations through simulation and graphical results.

5.2. System Description

The studied manipulator is a planar arm composed of two rigid links **Figure 5.1** connected by two revolute joints. The motion of the arm is confined to a two-dimensional plane .

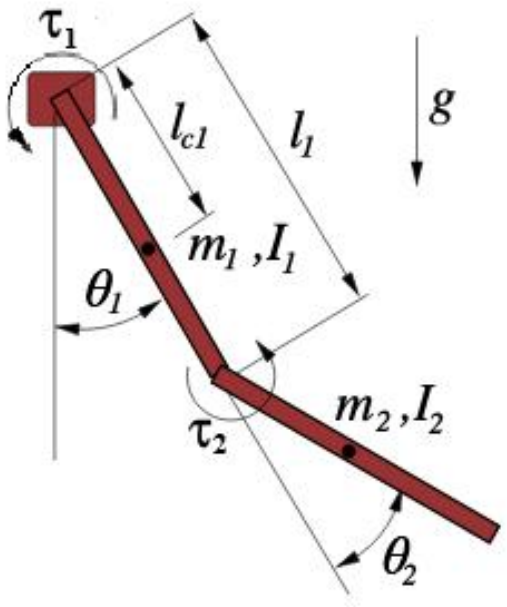

Figure 5.1: 2-DOF planar robot

Variables:

θ_1: The joint angle of Link 1

θ_2: The joint angle of Link 2

m_1: Mass of Link 1.

m_2: Mass of Link 2.

l_1: Length of Link 1.

l_2: Length of Link 2.

I_1: Moment of inertia of Link 1 about its center of mass.

I_2: Moment of inertia of Link 2 about its center of mass.

g: Acceleration due to gravity.

τ_1: Input torque at joint 1.

τ_2: Input torque at joint 2.

5.3. The 2-DOF planar robot dynamic modeling

Consider a planar robot with two links connected by revolute joints. Each link has a specific length, mass, and inertia [85].

1. **Link 1**: The first rigid segment attached to the base. This link is connected to **Joint 1** and can rotate around the base joint.
2. **Link 2**: The second rigid segment connected to **Link 1** by **Joint 2**. This link can rotate relative to **Link 1** around the elbow joint.
3. **Revolute Joints**: Both joints allow rotational movement. Joint 1 provides the rotation of **Link 1** around the base, while Joint 2 rotates **Link 2** relative to **Link 1**.

The motion of the arm can be described by the angles θ1 and θ2, which are the angular displacements of **Joint 1** and **Joint 2**, respectively.

For modeling the **dynamics** of a 2-DOF planar robot, we need to consider the forces and torques acting on the robot, as well as its motion. The dynamic equations can be derived using **Lagrangian mechanics**

5.3.1. Lagrangian Dynamics Model

The total kinetic energy T of the system consists of the translational kinetic energy of the center of mass of each link and the rotational kinetic energy of each link about its own center of mass.

$$T_1 = \frac{1}{2} I_1 \dot{q}_1^2 \qquad (5,1)$$

$$T_2 = \frac{1}{2}(I_2 + m_2 l_1^2 + 2m_2 l_1 l_{c2} c_2)\dot{q}_1^2 + \frac{1}{2} I_2 \dot{q}_2^2 + (I_2 + m_2 l_1 l_{c2} c_2)\dot{q}_1 \dot{q}_2 \qquad (5,2)$$

$$T = T_1 + T_2 \qquad (5,3)$$

$$\tau_1 = (I_1 + I_2 + m_2 l_1^2 + 2m_2 l_1 l_{c2} c_2)\ddot{q}_1 + (I_2 + m_2 l_1 l_{c2} c_2)\ddot{q}_2 - 2m_2 l_1 l_{c2} s_2 \dot{q}_1 \dot{q}_2 - 2m_2 l_1 l_{c2} s_2 \dot{q}_2^2 + m_1 g l_{c1} s_1 + m_2 g (l_1 s_1 + l_{c2} s_{1+2}) \qquad (5,4)$$

$$\tau_2 = (I_2 + m_2 l_1 l_{c2} c_2)\ddot{q}_1 + I_2 \ddot{q}_2 + m_2 l_1 l_{c2} s_2 \dot{q}_1^2 + m_2 g l_{c2} s_{1+2} \qquad (5,5)$$

The potential energy is due to the gravitational force acting on each link. Assuming gravity acts in the downward direction (along the negative y-axis)

$$U = -m_1 g l_{c1} c_1 - m_2 g (l_1 c_1 + l_{c2} c_{1+2}) \qquad (5,6)$$

The two equations represent the dynamics of the robot. For practical purposes, we typically express the system of equations in the following form:

We put : $q = [\theta_1 \quad \theta_2]^T, \tau = [\tau_1 \quad \tau_2]^T$

on obtient

$$\mathbf{M}(\mathbf{q})\ddot{\mathbf{q}} + C(q, \dot{q})\dot{q} + G(q) = \tau \qquad (5,7)$$

With :

$$\mathbf{M}(\mathbf{q}) = \begin{bmatrix} I_1 + I_2 + m_2 l_1^2 + 2m_2 l_1 l_{c2} c_2 & I_2 + m_2 l_1 l_{c2} c_2 \\ I_2 + m_2 l_1 l_{c2} c_2 & I_2 \end{bmatrix} \qquad (5,8)$$

$$\mathbf{C}(\mathbf{q}, \dot{\mathbf{q}}) = \begin{bmatrix} 2m_2 l_1 l_{c2} s_2 \dot{q}_2 & -m_2 l_1 l_{c2} s_2 \dot{q}_2 \\ m_2 l_1 l_{c2} s_2 \dot{q}_1 & 0 \end{bmatrix} \qquad (5,9)$$

$$\mathbf{G(q)} = \begin{bmatrix} m_1 g l_{c1} s_1 + m_2 g (l_1 s_1 + l_{c2} s_{1+2}) \\ m_2 g l_{c2} s_{1+2} \end{bmatrix} \tag{5,10}$$

Where:

- M: the **mass (inertia) matrix**.
- C: are the elements of the **Coriolis matrix**.
- G: are the elements of the **gravity vector**.

5.4.The Simulink Model for 2-DOF Arm manipulator Control

The simulator was built using MATLAB.

MATLAB provides powerful engineering tool including frequently used mathematical functions. It is easy to implement control algorithm including visualization of data used in the algorithm. In addition, by using Virtual Reality Toolbox, it is convenient to treat 3D objects defined with VRML (Virtual Reality Modeling Language). Thus, it is possible to build a simulator within a relatively short period. Virtual Reality (VR) is a system which allows one or more users to move and react in a computer generated environment. The basic VR systems allow the user to visual information using computer screens.

The simulation contains two parts.First, building model for 2-DOF arm manipulator,second, constitution of the simulink model in MATLAB then calling and running the model of arm using virtual reality toolbox.

Figure 5.2 shows the Block Diagram Schema for 2-DOF Manipulator Control System.

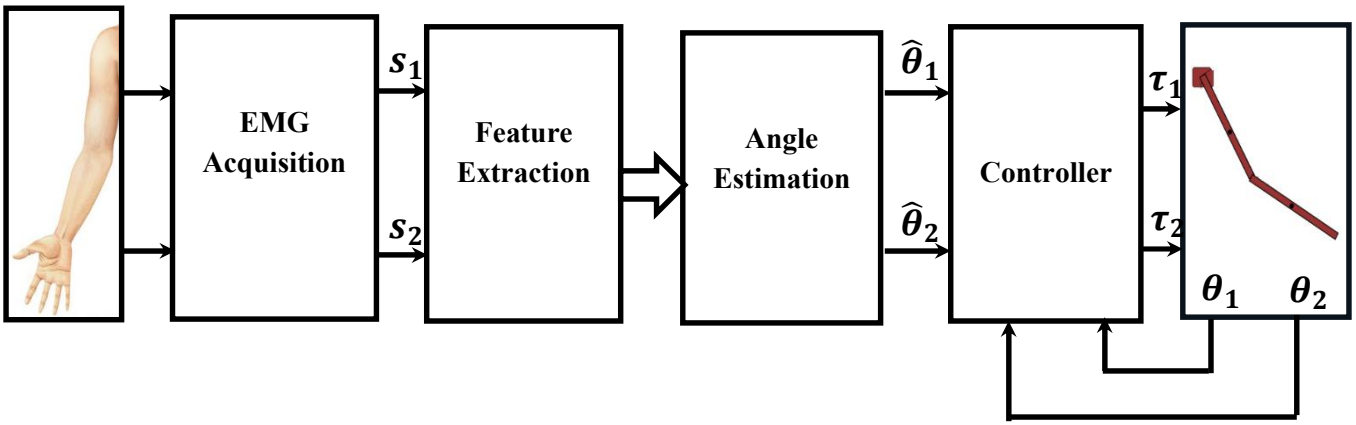

Figure 5.2: Block Diagram Schema for 2-DOF Manipulator Control System.

Figure 5.2 illustrates the block diagram of a control system for a two-degree-of-freedom (2-DOF) robotic manipulator.

After angle estimaton step:

The system begins with a desired joint Angles input, which specifies the reference angles for the two joints. This reference signal is compared with the measured joint angles obtained, producing a position error for each joint.

The error signals are fed into the controller, which computes the appropriate control torques required to drive the manipulator joints toward the desired positions. The controller incorporate proportional–integral–derivative (PID), model-based to compensate for system dynamics and disturbances. the equations of motion are:

$$\tau = \mathrm{M(q)\ddot{q}} + C(q,\dot{q})\dot{q} + G(q) \qquad (5,11)$$

joint angles : $q = [\theta_1 \quad \theta_2]^T$

joint torques ; $\tau = [\tau_1 \quad \tau_2]^T$

PID control equations:

$$\mathrm{e(t)=q_d\,(t) - q(t)} \qquad (5,12)$$

$$\mathrm{e(t)= K_p\, e(t) + K_d \frac{de(t)}{dt} + k_i \int e(t)\, i} \qquad (5,13)$$

with :

K_d : Derivative Gain

K_p : Proportional Gain

K_i : Integral Gain

The controller outputs are applied to the manipulator plant, which represents the nonlinear dynamic model of the 2-DOF robotic arm, including link inertia, Coriolis and centrifugal effects, gravity, and joint friction. The plant converts the applied torques into joint motions, resulting in actual joint angle.

Sensors measure the joint angles and feed this information back to the summing junction, forming a closed-loop feedback system. This feedback allows the controller to continuously correct deviations between the desired and actual joint angles, ensuring accurate trajectory tracking and stable operation of the manipulator.

5.5.Result and Simulation

- q1=O and (real q2) is commanded to follow (desired q2)

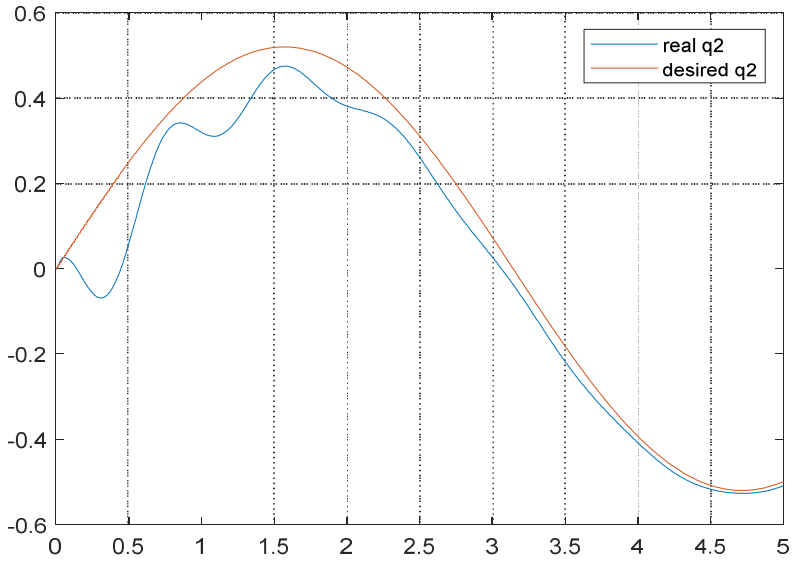

Figure 5.3: Joint Angle Tracking Results of q_2

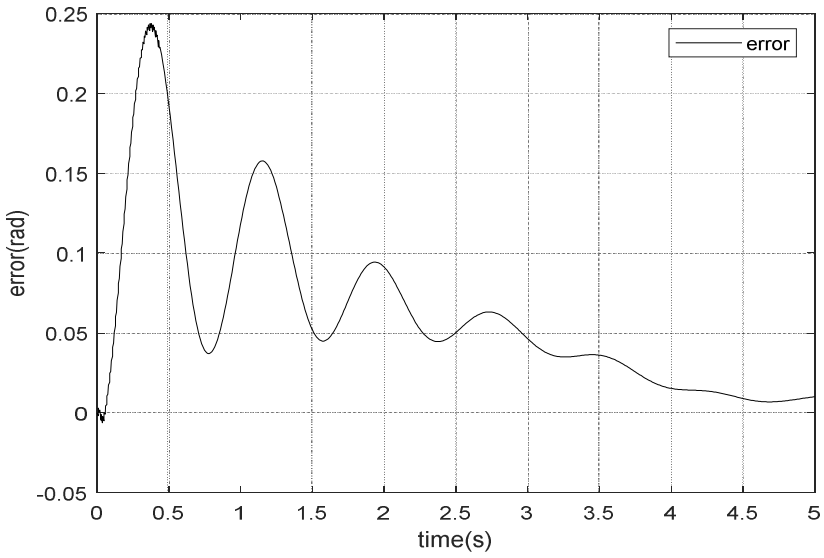

Figure 5.4: Error of joint Angle Tracking of q_2

The tracking error converges asymptotically to zero, confirming closed-loop stability

- (desired q2=0 and desired q1=0)

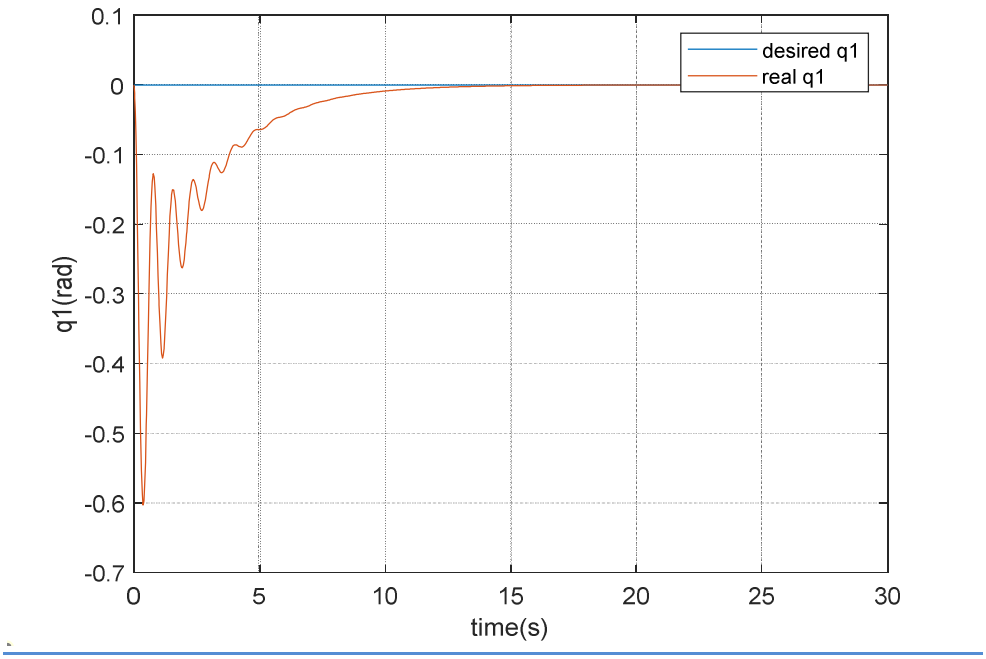

Figure 5.6: Joint Angle Tracking Results of q1=0rad.

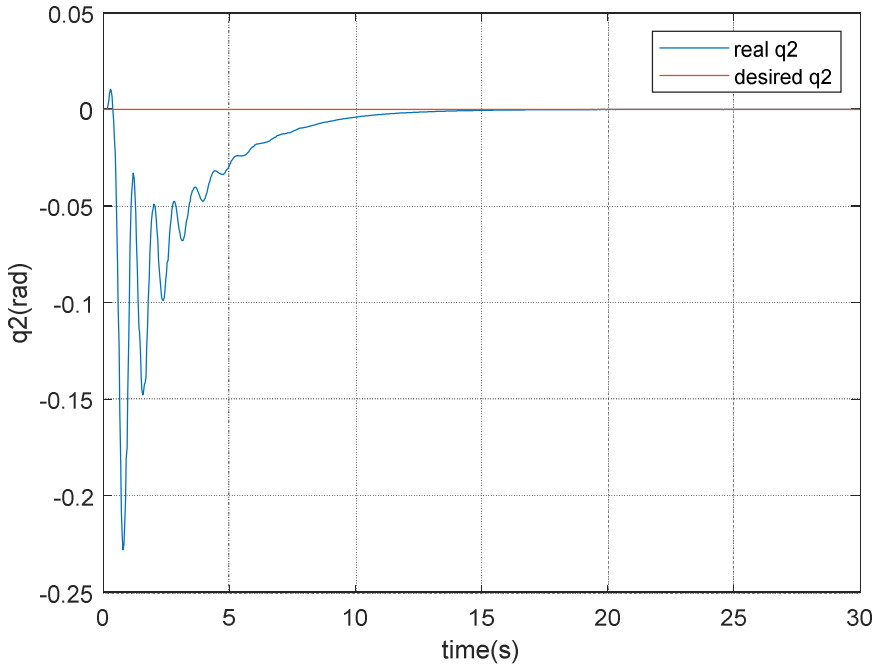

Figure 5.7: Joint Angle Tracking Results of q2=0rad.

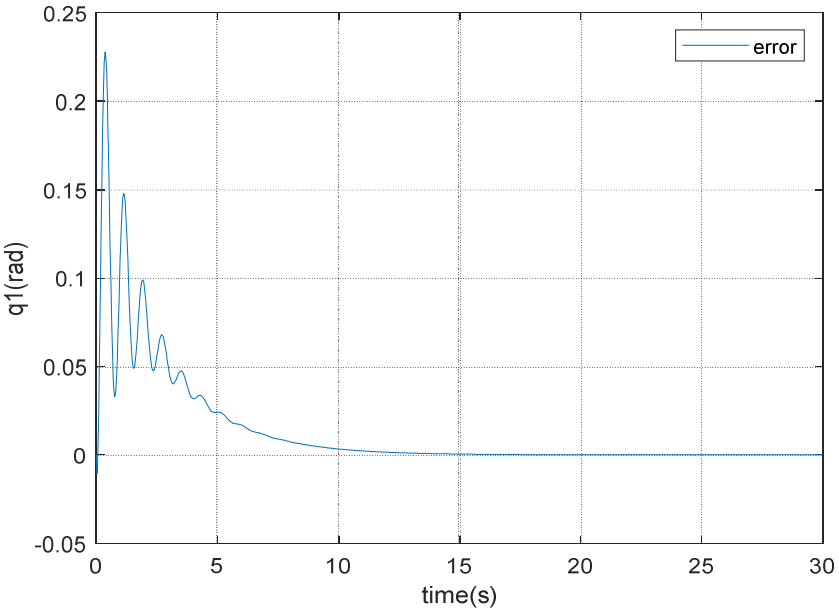

Figure 5.8 : Error of joint Angle Tracking of q1

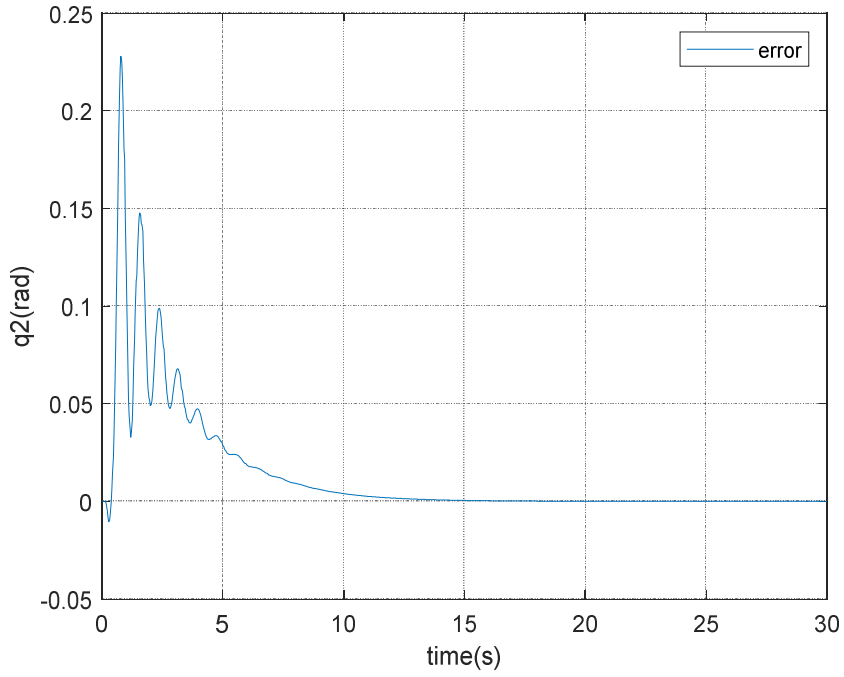

Figure 5.9 : Error of joint Angle Tracking of q_2

Simulation results demonstrate that the PID controller provides accurate trajectory tracking for both joints of the 2-DOF manipulator. The joint angles q1q_1q1 and q2q_2q2 closely follow their desired trajectories with minimal overshoot and zero steady-state error. The tracking errors converge to zero

5.6. Conclusion:

This chapter demonstrates the successful simulation of a 2-DOF planar manipulator using PID control in MATLAB/Simulink. The robot arm efficiently reaches the desired angles rotation while minimizing joint errors, and show the effectiveness of PID controllers for robotic applications.

Conclusion:

This thesis aimed to identify methods for categorizing EMG signals from the right forearm muscle, recorded by a MyoWare muscle sensor. The efficacy of diverse time domain and frequency domain characteristics in motion identification and classifier performance evaluation was assessed by analyzing the impact of extracted features and their combinations on classification accuracy. To attain the suggested objective, we segmented our effort into two primary phases.

In the first stage, an introduction to the EMG signal technique, feature extraction methods, and EMG Signal classification for Pattern Recognition were presented in three separate chapters. These chapters included the methodologies that will be utilized for our research.

The second stage involves the presentation of the materials and procedures that were utilized in order to gather the dataset by utilizing an EMG muscle sensor and the MPU6050 board. Following this, a method that is based on wavelets is proposed in order to evaluate EMG indicators. Following that, the extracted characteristics are presented in the form of feature vectors, which are then utilized by an LDA classifier in order to arrive at an estimate of the forearm flexion angles and to forecast the movement of the human forearm. Following this, a discussion of the findings of the study is presented; this stage was outlined in the previous chapter.

This study involved ten healthy participants who contributed to the collection of EMG data aimed at estimating the forearm angle flexion for four distinct gestures, utilizing linear discriminant analysis (LDA) and ANFIS as classifiers.

A MyoWare muscle sensor (AT-04-001) was connected to a digital oscilloscope (Hantek 6022BE) and the MPU6050 board, which communicated with an Arduino Uno, to acquire data from an EMG signal.

The mean absolute value, standard deviation, and root mean square features derived from the EMG signal and its discrete wavelet decomposition coefficients at level 2 (utilizing Debauchees 2 as the mother wavelet) were evaluated using the LDA classifier to identify relevant feature pairs.

The wavelet transform has been chosen to represent the EMG signal in the time-frequency domain due to its non-stationary nature.

The experimental findings indicate that the integrated RMS, MAV, and STD characteristics derived from the EMG signal have a high classification accuracy of 95%. The latter was enhanced by using the STD value derived from the wavelet decomposition coefficients (detail 2), achieving an accuracy of 97.50%.

The distinctive feature of this study was the utilization of user training data and testing with other users.

We were able to improve the classification accuracy by utilizing the recommended data acquisition protocol and a limited number of features.

In the future, we will endeavor to augment our dataset and utilize the current wavelet transform methodology to improve classification accuracy.

REFERENCES

[1] MOKHLESABADIFARAHANI, B., GUNJAN, V.K., ‘‘Introduction to EMG Technique and Feature Extraction’’, in EMG Signals Characterization in Three States of Contraction by Fuzzy Network and Feature Extraction, Springer, ed. 1, Singapore, 2015, pp. 1–9.

[2] MEENA P., MALTI BANSAL M., "Classification of EMG Signals Using SVM-kNN", in International Journal of Advanced Research in: Electronics and Communication Engineering (IJARECE), 2016, vol. 5, no. 6, pp. 1718–1724.

[3] SRAVANIA, C., BAJAJA, V., TARANA, S., SENGURB, A., "Flexible Analytic Wavelet Transform Based Features for Physical Action Identification Using sEMG Signals," in: IRBM, 2020, vol. 41, no. 1, pp. 18–22, ISSN 1959-0318.

[4] MILOSEV B., BENATTIV S., FARELLA E., "Design Challenges for Wearable EMG Applications," **Proceedings of the Design, Automation, and Test in Europe**, 2017, pp. 1432–1437.

[5] PRAKASH, A., BINDU, K., SHIRU, S., “A low-cost, wearable sEMG sensor for upper limb prosthetic application”, in Journal of Medical Engineering & Technology, 2019, vol. 43, no. 4, pp. 235-247, ISSN 0309-1902.

[6] FAJARDO, J., GOMEZ, O., PRIETO, F., “EMG hand gesture classification using handcrafted and deep features”, in Biomedical Signal Processing and Control, 2021, vol. 63, ISSN 1746-8094.

[7] CELANI N. M., SORIA C. M., OROSCO E. C., DI SCIASCIO F. A., VALENTINUZZI M. E., “Two dimensional myoelectric control of a robotic arm for upper limb amputees” , in: the 16th Argentine Bioengineering Congress and the 5th Conference of Clinical Engineering, San Juan, Argentina, 26-28 Sep. 2007.

[8] BALBINOT, A., FAVIEIRO, G., “A Neuro-Fuzzy System for Characterization of Arm Movements”, in sensors, 2013, Vol. 13, no. 2, pp. 2613-2630,ISSN 1424-8220.

[9] ORTES F., KARABULUT D., ZIYA ARSLAN Y., ‘‘General Perspectives on Electromyography Signal Features and Classifiers Used for Control of Human Arm Prosthetics’’, in Encyclopedia of Information Science and Technology, M. Khosrow-Pour editor, ed.4, Turkey, 2018, pp. 492-504.

[10] KARLSSON, S., GERDLE, B., "Mean frequency and signal amplitude of the surface EMG of the quadriceps muscles increase with increasing torque: a study using the continuous wavelet transform", in Journal of Electromyography and Kinesiology, 2001, vol. 11, pp. 131–140, ISSN 1050-6411.

[11] ELHARIRI E ., El-BENDARY N., HASSANNIEN A.E., "A hybrid classification model for EMG signals using a grey wolf optimizer and SVMs", The 1st International Conference on Advanced Intelligent, Egypt, 28-30 Nov. 2015, pp. 297–307.

[12] ADHAM R., ASFOUR S. S., "Continuous Wavelet Transform Application to EMG Signals Dduring Human Gait" in: ***Record of Thirty-Second Asilomar Conference on Signals, Systems and Computers***", 1998, vol. 1, pp. 325-329.

[13] VALENTINO, R., MICHIELETTO, S., SPOLAOR, F., SAWACHA, Z., PAGELLO, E., "Processing of sEMG signals for online motion of a single robot joint through GMM modelization", IEEE International Conference on Rehabilitation Robotics (ICORR), 2015, pp. 943-949.

[14] SHENG, X., LV, B., GUO, W., ZHU, X., "Common spatial-spectral analysis of EMG signals for multiday and multiuser myoelectric interface", in Biomed. Signal Process Control, 2019, vol. 53.

[15] CHOWDHURY, R., REAZ, M., ALI, M. A., ASHRIF, A. A., KALAIVANI, C., CHANG, T. G., "Surface Electromyography Signal Processing and Classification Techniques", Sensors, 2013, vol. 13, no. 9, pp. 12431–12466, ISSN1424-8220.

[16] BABA HAMED, A., BECHAR, H., CHIKH, M. A., "Simulation of Premature Ventricular Contraction using ModelSim Se 6.2c", in Electrotehnica, Electronica, Automatica (EEA), 2018, vol. 66, no. 4, pp. 118-124, ISSN 1582-5175.

[17] Ferris, D.P.; Gordon, K.E.; Sawicki, G.S.; Peethambaran, A. An improved powered ankle-foot orthosis using proportional myoelectric control. J. Gait Posture **2006**, 23, 425–428.

[18] Konrad, P. The ABC of EMG, A Practical Introduction to Kinesiological Electromyography; Noraxon Inc.: Scottsdale,
AZ, USA, 2005.

[19] Wan Daud, W.M.B.; Yahya, A.B.; Horng, C.S.; Sulaima, M.F.; Sudirman, R. Features Extraction of Electromyography Signals in Time Domain on Biceps Brachii Muscle; International Journal of Modeling and Optimization: Bucharest, Romania, 2013, Volume 3.

[20] Nazmi, N., Abdul Rahman, M. A., Yamamoto, S.-I., Ahmad, S. A., Zamzuri, H., & Mazlan, S. A. (2016). A Review of Classification Techniques of EMG Signals during Isotonic and Isometric Contractions. ***Sensors***, ***16***(8), 1304. https://doi.org/10.3390/s16081304

[21] Englehart, K.; Hudgin, B.; Parker, P.A. A wavelet-based continuous classification scheme for multifunction myoelectric control. IEEE Trans. Biomed. Eng. **2001**, 48, 302–311.

[22] Reaz, M.B.I.; Hussain, M.S.; Mohd-Yasin, F. Techniques of EMG Signal Analysis: Detection, Processing, Classification and Applications; Biological Procedures Online: London, UK, 2006.

[23] Chowdhury, R.H.; Reaz, M.B.I.; Ali, M.A.M. Surface Electromyography Signal Processing and Classification Techniques. Sensors **2013**, 13, 12431–12466.

[24] Nadzri, A.A.A.; Ahmad, S.A.; Marhaban, M.H.; Haslina, J. Characterization of surface electromyography using time domain features for determining hand motion and stages of contraction. Australas. Phys. Eng. Sci. Med. **2014**, 37, 133–137.

[25] Nardo, F.D.; Mengarelli, A.; Maranesi, E.; Burattini, L.; Fioretti, S. Assessment of the ankle muscle co-contraction during normal gait: A surface electromyography study. J. Electromyogr. Kinesiol. **2015**,25, 347–354.

[26] Ahmad, S.A.; Chappel, P.H. Surface EMG pattern analysis of the wrist muscles at different speeds of contraction. J. Med. Eng. Technol. **2009**, 33, 376–385.Review2 5, 6, 7, 36,8, 9-12,

[27] Mokhles abad ifarahani, Bita & Gunjan, Vinit. (2015). EMG Signals Characterization in Three States of Contraction by Fuzzy Network and Feature Extraction. 10.1007/978-981-287-320-0.

[28] Gerdle B, Karlsson S, Day S, Djupsjöbacka M (1999) Acquisition, Processing and Analysis of the Surface Electromyogram. Modern Techniques in Neuroscience. Chapter 26: 705-755. Eds: Windhorst U and Johansson H. Springer Verlag, Berlin.

[29] Duchêne J and Gouble F (1993) Surface electromyogram during voluntary contraction: Processing tools and relation to physiological events. Critical Reviews in Biomedical Engineering 21(4):313–397

[30] Stegeman, Dick & Hermens, Hermie. (2007). Standards for suface electromyography: The European project Surface EMG for non-invasive assessment of muscles (SENIAM).

[31] HAMZI M., BOUMEHRAZ M.,HASSANI R., “ Flexion Angle Estimation From Single Channel Forearm EMG Signals Using Effective Feature”, in *Electrotehnica, Electronica, Automatica* (*EEA*), 2023, vol. 69, no. 1, pp. 05-10, ISSN 1582-5175.

[32] FAJARDO, J., GOMEZ, O., PRIETO, F., “EMG hand gesture classification using handcrafted and deep features”, in Biomedical Signal Processing and Control, 2021, vol. 63, ISSN 1746-8094.

[33] BALBINOT, A., FAVIEIRO, G., “A Neuro-Fuzzy System for Characterization of Arm Movements”, in sensors, 2013, Vol. 13, no. 2, pp. 2613-2630, ISSN 1424-8220.

[34] Freriks B and Hermens H (2000) European Recommendations for Surface ElectroMyoGraphy, Results of the SENIAM Project (CD-rom). Roessingh Research and Development, The Netherlands

[35] Hewson DJ, Hogrel J-Y, Langeron Y, Duchêne J (2002) Evolution in impedance at the electrode-skin interface of two types of surface EMG electrodes during long-term recordings. Proceedings: XIVth Congress of the International Society of Electrophysiology and Kinesiology 173-174. Eds: Kollmitzer J and Bijak M. University of Vienna, Austria.

[36] Duff R, Nolan P, Rybansky M, O’Malley M. (2002) Evolution in impedance at the electrode-skin interface of two types of surface EMG electrodes during long-term recordings. Proceedings: XIVth Congress of the International Society of Electrophysiology and Kinesiology 175-176. Eds: Kollmitzer J and Bijak M. University of Vienna, Austria.

[37] Merletti R and Migliorini M (1998) Surface EMG electrode noise and contact impedance. Proceedings of the third general SENIAM workshop.

[38] Day SJ (1997) The Properties of Electromyogram and Force in Experimental and Computer Simulations of Isometric Muscle Contractions: Data from an Acute Cat Preparation. Dissertation, University of Calgary, Calgary.

[39] Ortes, F., Karabulut, D., & Arslan, Y. Z. (2019). General Perspectives on Electromyography Signal Features and Classifiers Used for Control of Human Arm Prosthetics. In M. Khosrow-Pour, D.B.A. (Ed.), *Advanced Methodologies and Technologies in Engineering and Environmental Science* (pp. 1-17). IGI Global Scientific Publishing. https://doi.org/10.4018/978-1-5225-7359-3.ch001

[40] PHINYOMARK, A., PHUKPATTARANONT, P., & LIMSAKUL,C. (2012). FEATURE REDUCTION AND SELECTION FOR EMG SIGNAL CLASSIFICATION. *EXPERT SYSTEMS WITH APPLICATIONS,* 39(8), 7420–7431. DOI:10.1016/J. ESWA.2012.01.102

[41] KALLENBERG, L. A. C., SCHULTE, E., DISSELHORST- KLUG, C., & HERMENSA, H. J. (2007). MYOELECTRIC MANIFESTATIONS OF FATIGUE AT LOW CONTRACTION LEVELS IN SUBJECTS WITH AND WITHOUT CHRONIC PAIN. *JOURNAL OF ELECTROMYOGRAPHY AND KINESIOLOGY*, 17(3), 264–274. DOI: 10.1016/J.JELEKIN.2006.04.004 PMID:16790358

[42] Khezri, M.; Jahed, M. A Neuro–Fuzzy Inference System for sEMG-Based Identification of Hand Motion Commands. IEEE Trans. Ind. Electron. **2007**, 58, 1952–1960.

[43] F. Marie, ``Wavelet transforms and their applications to turbulence," *Annu. Rev. Fluid Mech.*, vol. 24, pp. 395_457, Jan. 1992.

[44] I. W. Selesnick, ``Hilbert transform pairs of wavelet bases," *IEEE Signal Process. Lett.*, vol. 8, no. 6, pp. 170_173, Jun. 2001.

[45] I. W. Selesnick, ``The design of approximate Hilbert transform pairs of wavelet bases," *IEEE Trans. Signal Process.*, vol. 50, no. 5, pp. 1144_1152, May 2002.

[46] I. W. Selesnick, ``The design of Hilbert transform pairs of wavelet bases via the _at delay lter," in *Proc. IEEE Int. Conf. Acoust., Speech, Signal Process.*, May 2001, pp. 3673_3676.

[47] H. Ozkaramanli and R. Yu, ``On the phase condition and its solution for Hilbert transform pairs of wavelets bases," in *Proc. IEEE Int. Conf. Acoust., Speech, Signal Process. (ICASSP)*, Apr. 2003, p. 417.

[48] Y. Mallet, O. de Vel, and D. Coomans, ``Fundamentals of wavelet transforms," in *Wavelets in Chemistry* (Data Handling in Science and Technology), vol. 22, B.Walczak, Ed. Amsterdam, The Netherlands: Elsevier, 2000, pp. 57_84. [Online]. Available: https://www.sciencedirect.com/ science/article/pii/S0922348700800283

[49] Guo, T., Zhang, T., Lim, E., Lopez-Benitez, M., Ma, F., & Yu, L. (2022). A review of wavelet analysis and its applications: Challenges and opportunities. *IEEe Access*, *10*, 58869-58903.

[50] Uzunoğlu, C. P. (2018). A Comparative study of empirical and variational mode decomposition on high voltage discharges. *Electrica*, *18*(1), 72-77.

[51] Y. Lei, J. Lin, Z. He, M.J. Zuo, "A review on empirical mode decomposition in fault diagnosis of rotating machinery", *Mechanical Systems and Signal Processing*, vol.35, no.1, pp.108-126, 2013.

[52] D. P. Mandic, N. Rehman, Z. Wu, N. E. Huang, "Empirical mode decomposition- based time-frequency analysis of multivariate signals: The power of adaptive data analysis", *IEEE signal processing magazine*, vol. 30, no. 6, pp. 74-86, 2013.

[53] Dragomiretskiy, D. Zosso, "Variational Mode Decomposition", *in IEEE Transactions on Signal Processing*, vol. 62, no. 3, pp. 531-544, Feb. 1, 2014.

[54] Englehart, K.; Hudgins, B.; Parker, P.A.; Stevenson, M. Classification of the myoelectric signal using time-frequency based representations. Med. Eng. Phys. **1999**, 21, 431–438.

[55] Englehart, K.; Hudgin, B.; Parker, P.A. A wavelet-based continuous classification scheme for multifunction myoelectric control. IEEE Trans. Biomed. Eng. **2001**, 48, 302–311.

[56] Khushaba, R.N.; Al-Jumaily, A. Fuzzy Wavelet Packet Based Feature Extraction Method for Multifunction Myoelectric Control. Int. J. Biomed. Sci. **2007**, 3, 1–19.

[57] Ahsan, M.R.; Ibrahimy, M.; Khalifa, O. Neural Network Classifier for Hand Motion Detection from EMG Signal; Springer Berlin Heidelberg: Kuala Lumpur, Malaysia, 2011; pp. 536–541.

[58] Xie, H.B.; Guo, T.; Bai, S.; Dokos, S. Hybrid soft computing systems for electromyographic signals analysis: A review. BioMed. Eng. Online **2014**, 13, 1–19.

[59] Ahmad, S.A. Moving Approximate Entropy and its Application to the Electromyographic Control of an Artificial Hand. Ph.D. Thesis, University of Southamptom, Southampton, UK, 2009.

[60] Hussein, S.E.; Granat, M. Intention detection using a neuro-fuzzy EMG classifier. IEEE Eng. Med. Biol. **2002**, 21, 123–129.

[61] Vapnik, V. The Nature of Statistical Learning Theory; Springer: New York, NY, USA, 2000.

[62] Subasi, A. Classification of EMG signals using PSO optimized SVM for diagnosis of neuromuscular disorders. Comput. Biol. Med. **2013**, 43, 576–586.

[63] Zadeh, L. A. (1973). Outline of a new approach to the analysis of complex systems and decision process. *IEEE Transactions on Systems, Man, and Cybernetics*, *SMC-3*(1), 28–44. doi:10.1109/ TSMC.1973.5408575

[64] Kiguchi, K., Tanaka, T., Watanabe, K., & Fukuda, T. (2003). Exoskeleton for human upper-limb motion support, *IEEE International Conference on Robotics and Automation*, 2206 – 2211.

[65] Leon, M., Gutierrez, J. M., Leija, L., & Munoz, R. (2011). EMG pattern recognition using support vector machines classifier for myoelectric control purposes. *Pan American Health Care Exchanges*
(PAHCE), 175–178.

[66] Lucas, M. F., Gaufriau, A., Pascual, S., Doncarli, C., & Farina, D. (2008). Multi-channel surface EMG classification using support vector machines and signal-based wavelet optimization. *Biomedical Signal Processing and Control*,

[67] Arslan, Y. Z., Adli, M. A., Akan, A., & Baslo, M. B. (2010). Prediction of externally applied forces to human hands using frequency content of surface EMG signals. *Computer Methods and Programs in Biomedicine*, *98*(1), 36–44. doi:10.1016/j. cmpb.2009.08.005 PMID:19762107

[68] Chan, F. H. Y., Yang, Y. S., Lam, F. K., Zhang, Y. T., & Parker, P. A. (2000). Fuzzy EMG classification for prosthesis control. *IEEE Transactions on Rehabilitation Engineering*, *8*(3), 305–311. doi:10.1109/86.867872 PMID:11001510

[69] Chu, J. U., Moon, I., Lee, Y. J., Kim, S. K., & Mun, M. S. (2007). A supervised feature projection based real-time EMG pattern recognition for multifunction myoelectric hand control. *IEEE/ASME Transactions on Mechatronics*, *12*(3), 282–290. doi:10.1109/TMECH.2007.897262

[70] Phinyomark, A., Quaine, F., Charbonnier, S., Serviere, C., Tarpin-Bernard, F., & Laurillau, Y. (2013). EMG feature evaluation for improving myoelectric pattern recognition robustness. *Expert Systems with Applications*, *40*(12), 4832–4840. doi:10.1016/j.eswa.2013.02.023

[71] Subasi, A. (2012). Classification of EMG signals using combined features and soft computing techniques. *Applied Soft Computing*, *12*(8), 2188–2198. doi:10.1016/j.asoc.2012.03.035

[72] GRAUPE, D., SALAHI, J., KOHN, K. H., "Multifunctional prosthesis and prosthesis control via microcomputer identification of temporal pattern differences in single-site myoelectric signals'', in J. Biomed. Eng, 1982, vol. 4, no. 1,pp. 17–22.

[73] 3-lead Muscle / Electromyography Sensor for Microcontroller Applications, viewed on 2015, retrieved form: https://www.mouser.com/datasheet/2/813/MyowareUserManualAT-04-001-1223951.pdf.

[74] BENDIB, H., BAHRI, M., BOUMEHRAZ, M., MALLEM, A., HAMZI, M., “Implementation of a New Versatile Bio-Potential Measurement System”, in Journal of Circuits Systems and Computers, 2022, vol. 32, no. 8, ISSN 02018-1266.

[75] TELLI, K., BOUMEHRAZ, M., “Black-Box System Identification for Low-Cost Quadrotor Attitude at Hovering”, in Electrotehnica, Electronica, Automatica (EEA), 2022, vol. 70, no. 4, pp. 88-97, ISSN 1582-5175.

[76] HASSANI, R., BOUMEHRAZ, M., HAMZI, M., HABBA, Z., “Gyro-Accelerometer based Control of an Intelligent Wheelchair”, in Journal of Applied engineering Science and Technology(JAEST) , 2018, vol. 4, no. 1, pp. 101-107, ISSN 2352-9873.

[77] HASSANI R., “Multimodal Control of an Intelligent Wheelchair”, doctoral thesis in science, October 14, 2020, Algeria.

[78] VALENTINO, R., MICHIELETTO, S., SPOLAOR, F., SAWACHA, Z., PAGELLO, E., “Processing of sEMG signals for online motion of a single robot joint through GMM modelization”, IEEE International Conference on Rehabilitation Robotics (ICORR), 2015, pp. 943-949.

[79] TOO J., ABDULLAH A.R., TENGKU ZAWAWI T.N.S., MOHD SAAD N., MUSA H., “Classification of EMG Signal Based on Time Domain and Frequency Domain Features”, in International Journal of Human and Technology Interaction , 2017, vol. 1, no. 1, ISSN 2590-3551.

[80] NARAYAN Y., “ Hb vsEMG signal classification with time domain and Frequency domain features using LDA and ANN classifier” Proceedings of the International Conference on Newer Trends and Innovation in Mechanical Engineering: Materials Science, October 2020

[81] FAJARDO, J., GOMEZ, O., PRIETO, F., “EMG hand gesture classification using handcrafted and deep features”, in Biomedical Signal Processing and Control, 2021, vol. 63, ISSN 1746-8094.

[82] CHEN Z., ZHANG N., WANG Z., ZHOU Z., HU D., “ Hand gestures recognition from multi-channel forearm EMG signals”, International Conference on Cognitive Systems and Signal Processing, 2017, pp. 119-125.

[83] ZHANG, H., YANG, D., SHI, C., JIANG, L., LIU, H., “EMG pattern recognition with electrode donning/doffing and multiple confounding factors”, in Lecture Notes in Computer Science LNAI, 2017 ,vol. 10464, pp. 413-424.

[84] SHENG, X., LV, B., GUO, W., ZHU, X., “Common spatial-spectral analysis of EMG signals for multiday and multiuser myoelectric interface”, in Biomed. Signal Process Control, 2019, vol. 53.

[85] bukya, mohan. (2019). Modelling and Optimal control of Two link planar arm.